

1 A natural genetic variation screen identifies insulin signaling, neuronal communication, and
2 innate immunity as modifiers of hyperglycemia in the absence of *Sirt1*

3

4 Katie G. Owings* and Rebecca A.S. Palu†

5 *Department of Human Genetics, University of Utah School of Medicine, Salt Lake City, UT

6 84112

7 †Biology Department, Purdue University-Fort Wayne, Fort Wayne, IN 46818

8

9

10

11

12

13

14

15

16 **Running title: Natural modifiers of hyperglycemia**

17 **Key words: hyperglycemia, *Drosophila*, genetic variation, modifier genes**

18

19 Corresponding author:

20 Rebecca A.S. Palu

21 Biology Department

22 Science Building SB330

23 2101 E. Coliseum Blvd

24 Fort Wayne IN, 46805

25 260-481-5704

26 palur@pfw.edu

27

ABSTRACT

28 Variation in the onset, progression, and severity of symptoms associated with metabolic
29 disorders such as diabetes impairs the diagnosis and treatment of at-risk patients. Diabetes
30 symptoms, and patient variation in these symptoms, is attributed to a combination of genetic
31 and environmental factors, but identifying the genes and pathways that modify diabetes in
32 humans has proven difficult. A greater understanding of genetic modifiers and the ways in which
33 they interact with metabolic pathways could improve the ability to predict a patient's risk for
34 severe symptoms, as well as enhance the development of individualized therapeutic
35 approaches. In this study we use the *Drosophila* Genetic Reference Panel (DGRP) to identify
36 genetic variation influencing hyperglycemia associated with loss of *Sirt1* function. Through
37 analysis of individual candidate functions, physical interaction networks, and Gene Set
38 Enrichment Analysis (GSEA) we identify not only modifiers involved in canonical glucose
39 metabolism and insulin signaling, but also genes important for neuronal signaling and the innate
40 immune response. Furthermore, reducing the expression of several of these candidates
41 suppressed hyperglycemia, making them ideal candidate therapeutic targets. These analyses
42 showcase the diverse processes contributing to glucose homeostasis and open up several
43 avenues of future investigation.

44

45

INTRODUCTION

46 Metabolic diseases, and in particular diabetes, are one of the most pressing health crises in the
47 developed world, with incidences continuing to rise in the last 20 years (CDC 2020). 37.7% of
48 adults in the US are diagnosed as obese and 10.5% as having some form of diabetes, and it is
49 estimated that millions more go undiagnosed (Flegal *et al.* 2016; CDC 2020). What is more, the
50 monetary cost of these disorders to the public has grown to astronomical levels. It is estimated
51 that \$237 billion in direct costs and at least \$90 billion in indirect costs were spent on healthcare
52 related to diabetes and its various complications in 2017 alone, up ~25% from 2012 (Flegal *et*

53 *al.* 2016). A focused effort has been made to understand both the genetic and environmental
54 contributors to metabolic homeostasis, as well as to the disruption of that homeostasis that
55 leads to disease (Barroso and McCarthy 2019).

56
57 Unfortunately, even identifying these contributors has proven difficult. Metabolic diseases are
58 complex, and the onset, progression, and ultimately the severity of any individual case is
59 dependent upon a myriad of genetic and environmental variables and the ways in which they
60 interact with one another (Queitsch *et al.* 2012; Barroso and McCarthy 2019). Even when there
61 is a strong familial link, phenotypic heterogeneity in disease phenotypes can make it difficult to
62 identify at-risk patients or make accurate prognostic predictions (Udler *et al.* 2019). This is
63 particularly true when it comes to predicting complications of diabetes such as neuropathy,
64 retinopathy, or kidney disease (Barroso and McCarthy 2019; Cabrera *et al.* 2020). Much of this
65 variation is due to inter-individual differences in genetic background, including silent cryptic
66 genetic variation that is revealed upon disease or stress (Queitsch *et al.* 2012; Chow 2016;
67 Barroso and McCarthy 2019).

68
69 One example of this kind of symptom heterogeneity can be observed in disease associated with
70 the deacetylase *SIRT1*. This highly conserved gene was originally identified as a histone
71 deacetylase important in heterochromatin formation in yeast (Shore *et al.* 1984; Ivy *et al.* 1986;
72 Rine and Herskowitz 1987). Since then, SIRT1 and its paralogs (the sirtuins) have been found
73 to have a number of additional targets, many of which are transcription factors and enzymes
74 with key roles in metabolic homeostasis (Brunet *et al.* 2004; Picard *et al.* 2004; Rodgers and
75 Puigserver 2007; Li *et al.* 2007; Yang *et al.* 2009; Palu and Thummel 2016). Importantly, as part
76 of their enzymatic reaction, sirtuins consume the cofactor NAD, which also serves as an
77 electron carrier in central metabolic pathways such as glycolysis and the TCA cycle. Sirtuin
78 enzymatic activity, therefore, is directly linked to the availability of this cofactor and thus is

79 responsive to the energetic state of the cell. This information is then conveyed to the targets,
80 whose acetylation state alters their activity and stability in the cell (Nogueiras *et al.* 2012). With
81 this centralized role in regulating the response of metabolic factors to cellular energy availability,
82 it is unsurprising that variation in *SIRT1* has been linked to, among other things, the
83 development of diabetes (Zillikens *et al.* 2009; Botden *et al.* 2012; Biason-Lauber *et al.* 2013;
84 Zhao *et al.* 2017).

85
86 Elucidating the mechanism behind this link, however, has proven difficult. Loss-of-function and
87 gain-of-function studies in model systems have demonstrated a clear role for SIRT1 in
88 metabolic homeostasis, but the actual impacts on the animals in question have frequently been
89 contradictory (Boutant and Cantó 2014). It is likely that at least some of these contradictory
90 results stem from differences in genetic background between the animals used in the various
91 studies. Understanding the role of this variation and the genes or pathways which modify
92 metabolic disease will enable the development of improved diagnosis, prediction of prognosis,
93 and personalized treatment strategies for patients.

94
95 Model organism tools, such as the *Drosophila* Genetic Reference Panel (DGRP), provide a way
96 to study of the impact of natural genetic variation on diseases such as diabetes (Mackay *et al.*
97 2012; He *et al.* 2014; Ivanov *et al.* 2015; Nelson *et al.* 2016; Jehrke *et al.* 2018; Everman *et al.*
98 2019). The DGRP is a collection of ~200 isogenic strains derived from a wild population, such
99 that each strain represents one wild-derived genome (Mackay *et al.* 2012). The variation in the
100 DGRP is well tolerated under healthy, non-disease conditions and allows for the identification of
101 genetic polymorphisms that are associated with phenotypic variation in models of human
102 disease (Chow and Reiter 2017). Importantly, the availability of full-genome sequence for these
103 strains allows for genome-wide association analyses that link quantitative phenotypes with
104 genetic variation and modifier genes.

105

106 The utility of the DGRP in identifying candidate modifiers of metabolic disease has already been
107 demonstrated numerous times, with screens associated with misfolded insulin, high sugar and
108 high fat feeding, and starvation resistance already documented (Mackay *et al.* 2012; He *et al.*
109 2014; Ivanov *et al.* 2015; Nelson *et al.* 2016; Jehrke *et al.* 2018; Everman *et al.* 2019). While
110 some of these used biochemical assays to precisely measure metabolite levels in flies as a
111 quantitative phenotype for the screen (Nelson *et al.* 2016; Jehrke *et al.* 2018; Everman *et al.*
112 2019), several used more general physiological measurements such as starvation resistance
113 and lifespan (Mackay *et al.* 2012; Ivanov *et al.* 2015). Although effective, the use of this kind of
114 general readout reduces the specificity of the modifiers identified. Many genetic factors impact
115 survival and could lead to a high background signal. The same could be true for otherwise wild-
116 type flies subjected to different environmental conditions, even when more precise assays are
117 used as a quantitative phenotype (Nelson *et al.* 2016). A multitude of pathways and processes
118 impact the response to dietary changes through feeding rate, hormone secretion, anabolism
119 and catabolism rates, and nutrient absorption. Using a specific genetic model of disease and
120 then focusing on a specific phenotype, such as hyperglycemia, may reduce some of the noise
121 and increase specificity of the modifiers identified.

122

123 Furthermore, recent studies using the DGRP have demonstrated that the top candidate modifier
124 genes and pathways differ when different but related models of genetic disease are screened
125 (Chow *et al.* 2016; Palu *et al.* 2019). These results reinforce the idea that different causative
126 genes and mutations will interact with different pathways over the course of disease. It also
127 highlights the importance of exploring multiple disease models in something so diverse as
128 diabetes, and the utility of the DGRP in precisely distinguishing modifiers of a particular
129 genotype-phenotype combination.

130

131 In this study, we report the results of a natural variation screen in a model of *Sirt1* loss-of-
132 function. Loss of this gene in *Drosophila* has been shown to lead to progressive metabolic
133 dysfunction including obesity, hyperglycemia, and ultimately insulin resistance (Palu and
134 Thummel 2016). Our study design is specifically focused on the phenotype of hyperglycemia
135 when *Sirt1* expression is disrupted using RNAi in the adipose and liver-like fat body organ. We
136 observed substantial phenotypic variation across the DGRP for hyperglycemia associated with
137 loss of *Sirt1*. Using genome-wide association analysis, pathway enrichment, and the generation
138 of a physical interaction network, we identified a number of modifying pathways and processes,
139 several of which have known roles in central carbon metabolism, the immune response, and the
140 kind of neuronal signaling and communication expected to influence the neuroendocrine cells
141 responsible for insulin secretion in *Drosophila*. Finally, we confirmed that loss of several of the
142 top candidate modifier genes significantly alters glucose levels in the *Sirt1* RNAi model. Our
143 findings highlight exciting new areas of study for modifiers of *Sirt1* function, glucose
144 homeostasis, and insulin sensitivity.

145

146

METHODS

Fly stocks and maintenance

148 Flies were raised at room temperature on a diet based on the Bloomington Stock Center
149 standard medium with malt. Experimental crosses were maintained on a media containing 6%
150 yeast, 6% dextrose, 3% sucrose, and 1% agar, with 0.6% propionic acid and 0.1% p-Hydroxy-
151 benzoic acid methyl ester in 95% ethanol included as antifungal agents. Flies subjected to an
152 overnight fast were transferred to media containing only 1% agar in water. The *R4>Sirt1i* strain,
153 which serves as the model of hyperglycemia in this study, is derived from an *R4-GAL4* strain
154 (BDSC 33832) outcrossed to *w¹¹¹⁸* (Palu and Thummel 2016) and a *Sirt1* RNAi strain from the
155 Bloomington Stock Center (32481). 185 strains from the DGRP were used for the modifier
156 screen (Tables S1-S3), wherein virgin females carrying the *R4>Sirt1i* model were crossed to

157 males of the DGRP strains. Male F1 progeny carrying *R4>Sirt1i* were separated and aged for
158 one to two weeks. These flies were then either collected under ad libitum fed conditions or
159 fasted overnight and then collected. The following RNAi and control strains are from the
160 Bloomington Stock Center: *CG4168* RNAi (28636), *CG5888* RNAi (62175), *uif* RNAi (38354),
161 *CTPSyn* RNAi (31924), *smt3* RNAi (36125), *ilp5* RNAi (33683), *Vha55* RNAi (40884), *snRNP-*
162 *U1-70k* RNAi (33396), *CG10265* RNAi (43294), *CG15803* RNAi (51449), *Roe* RNAi (57836),
163 *CG34353* RNAi (58291), *CadN2* RNAi (27508), *Ace* RNAi (25958), *CG43897* (31560), *dsxc73A*
164 RNAi (56987), *bgm* RNAi (56979), *CG3407* RNAi (57762), control *attP40* (36304), and control
165 *attP2* (36303).

166

167 *Glucose Assay*

168 Samples of five flies each were collected at one or two weeks of age and washed in 1XPBS.
169 Samples were then either frozen in liquid nitrogen and stored long-term at -80C or immediately
170 homogenized in 100 uL 1X PBS. Frozen samples were kept frozen until immediately upon
171 addition of PBS and homogenization. After homogenization samples were subjected to heat
172 inactivation of enzymes at 70C for approximately 10 minutes. Glucose was measured undiluted
173 from the lysate using the Sigma HK Glucose Assay kit as described (Tennesen *et al.* 2014).

174

175 *Protein Assay*

176 Prior to heat inactivation, 10 uL of the fly lysate isolated for glucose measurement was saved
177 and kept on ice. Protein samples could then be stored long term at -80°C. Samples were
178 centrifuged for up to 5 minutes at room temperature and protein measured from the supernatant
179 after a 1:10 dilution using the Sigma Protein Assay Reagent as described (Tennesen *et al.*
180 2014).

181

182 *Phenotypic analysis and genome-wide association*

183 For each DGRP line, glucose was measured from 3 samples of 5 flies each. The P-values for
184 association of genetic background and glucose concentration were calculated using one-way
185 ANOVA on R software taking into account all collected data points for each experiment.
186 Average glucose concentration was used for the genome-wide association (GWA). GWA was
187 performed as previously described (Chow *et al.* 2016; Palu *et al.* 2019). DGRP genotypes were
188 downloaded from the website, <http://dgrp.gnets.ncsu.edu/>. Non-biallelic sites were removed. A
189 total of 3,636,891 variants were included in the analysis. Mean eye glucose concentration for
190 555 samples representing 2775 DGRP/R4>Sirt1i F1 progeny were regressed on each SNP. To
191 account for cryptic relatedness (He *et al.* 2014; Huang *et al.* 2014), GEMMA (v. 0.94) (Zhou and
192 Stephens 2012) was used to both estimate a centered genetic relatedness matrix and perform
193 association tests using the following linear mixed model (LMM):

$$y = \alpha + x\beta + u + \epsilon$$

$$u \sim \text{MVN}_n(0, \lambda \tau^{-1} K)$$

$$\epsilon \sim \text{MVN}_n(0, \tau^{-1} I_n)$$

197 where, as described and adapted from Zhou and Stephens 2012, y is the n -vector of average
198 glucose concentration for the n lines, α is the intercept, x is the n -vector of marker genotypes, β
199 is the effect size of the marker. u is a $n \times n$ matrix of random effects with a multivariate normal
200 distribution (MVN _{n}) that depends on λ , the ratio between the two variance components, τ^{-1} ,
201 the variance of residual errors, and where the covariance matrix is informed by K , the
202 calculated $n \times n$ marker-based relatedness matrix. K accounts for all pairwise non-random
203 sharing of genetic material among lines. ϵ , is a n -vector of residual errors, with a multivariate
204 normal distribution that depends on τ^{-1} and I_n , the identity matrix. Quantile-quantile (qq)
205 plots demonstrate an appropriate fit to the LMM at the positive end of the plot, but a greater
206 number of points than expected by chance with an insignificant p -value (Figure S1). Genes
207 were identified from SNP coordinates using the BDGP R54/dm3 genome build. A SNP was
208 assigned to a gene if it was +/- 1 kb from a gene body.

209

210 *RNAi Validation*

211 Virgin females from the *R4>Sirt1i* model were crossed to males carrying RNAi constructs
212 targeting candidate modifiers of those models, and the glucose levels of F1 male progeny
213 expressing both *Sirt1i* and the modifier RNAi construct specifically in the fat body were
214 measured as described above on 4-5 samples of 5 male flies each. Glucose concentrations
215 from RNAi-carrying strains are compared directly to genetically matched *attP40* or *attP2*
216 controls using a Dunnett's multiple comparisons test. Glucose measurements are normalized to
217 the appropriate genetically matched controls. Normalized controls from individual experiments
218 are compared in Figure S2. Standard deviation did not significantly vary between controls for
219 individual experiments.

220

221 *Bioinformatics Analysis*

222 Genetic polymorphisms were associated with candidate genes within 1 kb of the polymorphism.
223 Information about candidate genes and their human orthologues was gathered from a number
224 of databases including Flymine, Flybase, OMIM, and NCBI. Physical interaction maps were
225 generated using the GeneMANIA plugin on Cytoscape (version 3.8.2) (Shannon *et al.* 2003;
226 Montojo *et al.* 2010). GSEA was run to generate a rank-list of genes based on their enrichment
227 for significantly associated polymorphisms. For GSEA analysis, polymorphisms within 1kb of
228 more than 1 gene were assigned to one gene based on a priority list of exon, UTR, intron, and
229 upstream or downstream. Genes were assigned to GO categories, and calculation of
230 enrichment score was performed as described (Subramanian *et al.* 2005). Categories with ES
231 scores > 0 (enriched for associated genes with low p-values), gene number > 3, and p-values
232 <0.05 were included in the final output.

233

234

RESULTS

235 *Glucose levels in R4>Sirt1i flies vary with genetic background in a consistent pattern across*
236 *multiple conditions*

237 Loss of *Sirt1* expression leads to progressive hyperglycemia, obesity, and insulin resistance. To
238 model the hyperglycemia that is commonly associated with diabetes, we reduced the
239 expression of the deacetylase *Sirt1* specifically in the fat body of *Drosophila melanogaster*.
240 RNAi targeting *Sirt1* specifically in the fat body reproduces the hyperglycemia phenotype, with
241 an approximately 50-60% increase in whole fly glucose levels (P = 0.02, Figure S3) (Palu and
242 Thummel 2016). The fat body in *Drosophila* performs functions normally undertaken by the
243 adipose and liver tissues in humans (Géminard *et al.* 2009; DiAngelo and Birnbaum 2009;
244 Arrese and Soulages 2010). While there are likely roles for *Sirt1* in other metabolic tissues, its
245 function in the fat body clearly contributes to the maintenance of glucose homeostasis and
246 insulin sensitivity over time (Palu and Thummel 2016). Modifiers of insulin signaling or glucose
247 metabolism could alter the degree of hyperglycemia in this model.

248
249 The degree of hyperglycemia is determined by a biochemical assay that measures the
250 concentration of glucose in a whole-fly lysate (Tennessen *et al.* 2014). This is a quantitative
251 assay where higher concentrations of glucose correlate with more severe hyperglycemia, and
252 lower concentrations of glucose correlate with milder disease, or potentially hypoglycemia.

253 Glucose was measured specifically in males, as adult female *Drosophila* devote much of their
254 physiological output to egg production (Millington and Rideout 2018). Previous studies have
255 demonstrated that adult males provide a consistent model for metabolic homeostasis in the fly
256 (Sieber and Thummel 2009; Tennessen *et al.* 2014; Palu and Thummel 2016; Barry and
257 Thummel 2016; Beebe *et al.* 2020).

258
259 Loss of *Sirt1* is induced using the *GAL4/UAS* system, where *R4-GAL4* drives expression of
260 *UAS-Sirt1* RNAi (Figure S4A). *R4-GAL4* is strongly expressed primarily in the fat body of fly,

261 starting in early development and continuing through adulthood (Lee and Park 2004). The line
262 containing this model (*R4>Sirt1i*) serves as the donor strain that was crossed to each DGRP
263 strain. Females from the donor strain were crossed with males of each of 185 DGRP strains to
264 generate F1 progeny lacking *Sirt1* expression in the fat body. The progeny received 50% of their
265 genome from the maternal donor strain and 50% from the paternal DGRP strain (Figure S4B).
266 Therefore, we are measuring the dominant effect of the DGRP background on the *Sirt1* RNAi
267 hyperglycemia phenotype. This experimental design is similar to a model of *NGLY1* deficiency
268 using RNAi that was also crossed to the DGRP (Talsness *et al.* 2020).

269
270 In the prior study characterizing the impact of the loss of function of *Sirt1* on metabolic
271 homeostasis, the dysfunction observed was progressive in nature. While larvae and young
272 adults are immediately obese, hyperglycemia and insulin resistance set in and become worse
273 with increasing age (Reis *et al.* 2010; Palu and Thummel 2016). To ensure an appropriate set of
274 conditions with respect to diet and age, we performed a preliminary analysis on 37 DGRP
275 strains at one or two weeks of age, and under fasted or ad libitum fed conditions (Table S1).
276 These time points correspond to conditions in the original study where differences in the
277 metabolic state of the flies corresponded to differences in glycemia (Palu and Thummel 2016).
278 We wished to select a time point at which hyperglycemia was detectable, but also differed
279 enough between strains to allow us to identify genetic variation associated with that
280 heterogeneity.

281
282 Three samples were collected for glucose measurements in each strain and condition. Glucose
283 levels vary across genetic background for each of the conditions being tested (Figure 1A-D).
284 Average glucose for each strain is significantly correlated between one and two week fasted
285 flies ($R = 0.53$, $P = 4E-03$), between one-week-old fed and fasted flies ($R = 0.45$, $P = 0.020$),
286 and between one-week-old fed and two-week-old fasted flies ($R = 0.62$, $P = 2E-04$) (Figure

287 S5A-C). This supports glucose concentration as a consistent quantitative measurement.
288 Interestingly, evidence for correlation with two-week-old flies fed ad libitum is not as strong.
289 While a significant correlation is still detected with one-week-old fasted flies ($R = 0.43$, $P =$
290 0.014), the correlation is not significant with two-week-old fasted flies ($R = 0.25$, $P = 0.219$) and
291 one-week-old flies fed ad libitum ($R = 0.34$, $P = 0.063$) (Figure S5D-F). By two weeks of age,
292 *Sirt1* loss-of-function flies are beginning to experience more severe symptoms of disease, and
293 we expect to see variability in symptoms and behavior in response to those symptoms. Fed flies
294 at two weeks may have more variable glucose because feeding behavior is a big contributor to
295 glucose levels in flies that have not been subjected to a fast.

296

297 To identify the conditions under which the impact of genetic background was the strongest, we
298 performed a one-way ANOVA test that included all data points collected. We found that while
299 there is a significant association between glucose levels and genetic background under all
300 conditions ($p < 0.05$), this effect is most pronounced in the one-week-old flies fed ad libitum ($P =$
301 $1.87E-5$) and in the two-week-old fasted flies ($P = 1.95E-5$) (Figure 1A,D). Because fasting
302 reduces possible intra-strain variation caused by food in the gut, two weeks fasted was selected
303 for the full screen.

304

305 We examined protein concentrations in 90 samples from the first 30 strains collected at 2 weeks
306 fasted to ensure that any variation we observe in glucose is not due to differences in body size.
307 Protein levels do not significantly vary across the DGRP ($P = 0.63$, Figure S6A), nor do protein
308 levels correlate with glucose levels in individual samples ($R = 0.04$, $P = 0.6577$, Figure S6B).
309 We conclude that the variation we observe in fasting glucose levels are due to differences in
310 circulating glucose, and not to differences in body size.

311

312 *Genome-wide association analysis identifies candidate modifiers of Sirt1i-associated*
313 *hyperglycemia*

314 Using the conditions determined in the preliminary screen, we proceeded to cross the donor
315 strain with the remaining 149 DGRP strains (Figure 2, Tables S2,S3). We found a significant
316 effect of genetic background on glycemia in the R4>Sirt1i flies ($P < 2E-16$) using one-way
317 ANOVA including all data points for each strain ($N = 555$). Individual glucose measurements
318 ranged from 0.306 $\mu\text{g}/\text{fly}$ to 3.416 $\mu\text{g}/\text{fly}$ (Table S2), while average concentrations ranged from
319 0.395 $\mu\text{g}/\text{fly}$ (RAL 801) to 2.438 $\mu\text{g}/\text{fly}$ (RAL 357) (Figure 2, Table S3).

320
321 To identify genetic polymorphisms that may be responsible for this observed variation in
322 glycemia, we performed a genome-wide association analysis. Average glucose level for each
323 strain was used as a quantitative phenotype to test for association with polymorphisms in the
324 DGRP. A total of 3,636,891 variants were tested for the R4>Sirt1i model across 186 lines. This
325 analysis as a result is insufficiently powered for candidates to remain statistically significant after
326 multiple testing corrections. Instead, the focus is on identification of candidate modifiers and
327 pathways that can be validated through further study and that will provide the basis for future
328 projects. This approach has been quite successful in previous studies (Chow *et al.* 2013, 2015,
329 2016; Palu and Chow 2018; Lavoy *et al.* 2018; Palu *et al.* 2019, 2020; Talsness *et al.* 2020).

330
331 Because the analyzed F1 hybrids in this case were male and inherited their X chromosome from
332 the donor strain and not the DGRP strain, we do not include any X-linked variants in the
333 resulting candidate modifiers. Using an arbitrary cut-off of $P < 10^{-4}$, we identified 237
334 polymorphisms on the second and third chromosomes (Table S4). Of these 237, 62 were not
335 considered further as they were not within ± 1 kb of a candidate gene. The remaining 175
336 polymorphisms are associated with a total of 161 candidate genes (Table S5). 100 of these
337 polymorphisms are intronic, 29 are exonic with 6 producing non-synonymous changes to the

338 peptide and one a start-gain, 10 are located in the 5' or 3' untranslated regions, and 36 are
339 within 1 kb up or downstream of the candidate gene (Table S4). Of note in this analysis is that
340 the results were not filtered for allele frequency > 0.05. This was a concerted choice; several of
341 the most interesting candidates, including *CG5888* and *ilp5*, would otherwise have been left out
342 of the analysis. The number of total variants analyzed drops from 237 to 90, and the number of
343 candidate genes associated at $P < 10^{-4}$ drops from 161 to 75. While this, along with the use of a
344 low stringency p-value cut-off, increases the probability of false positives, it likewise increases
345 our power when performing pathway enrichment. Validation of candidate genes with low minor
346 allele frequencies in later studies will distinguish true positives from false positives.

347
348 One concern with using an RNAi model to reduce *Sirt1* expression is that the modifiers
349 identified might be specific RNAi efficacy, rather than hyperglycemia. The modifiers could be
350 altering the degree and efficiency of *Sirt1* knockdown, so that hyperglycemia is actually
351 correlating with the amount of *Sirt1* expression that is achieved. If this were the case, we would
352 expect to see the top candidate modifiers associated with RNAi machinery or the efficiency of
353 the GAL4/UAS system. This does not appear to be the case, either from a single-gene function
354 perspective or when looking at enriched gene categories (Tables S5 and S6). Furthermore, the
355 GAL4/UAS system is commonly used to model disease in the DGRP, and the candidates
356 identified have always been unique to the disease and, at times, even the specific model in
357 question (He *et al.* 2014; Chow *et al.* 2016; Lavoy *et al.* 2018; Palu *et al.* 2019; Talsness *et al.*
358 2020). All of this suggests that the candidate genes identified through this screen are modifying
359 *Sirt1*-associated hyperglycemia directly rather than altering the degree of *Sirt1* knockdown.

360
361 *Candidate modifiers of Sirt1 are involved in basic metabolic processes, the immune response,*
362 *and the regulation of neuronal communication*

363 Because loss of *Sirt1* in the fat body alters glucose metabolism and insulin sensitivity in the
364 organism, we expected modifiers of hyperglycemia to impact pathways linked to central carbon
365 metabolism as well as external processes that influence secretion and signaling of hormones
366 such as insulin. To determine if this is the case, we examined the individual functions of the top
367 GWA candidates and looked for pathways and processes that are enriched in this list. While we
368 attempted first to do this through Gene Ontology analysis of our top candidates, we found no
369 significantly enriched terms. We therefore utilized individual known physical interactions and GO
370 term enrichment through GSEA to highlight likely candidate pathways.

371

372 **Analysis of Candidate Modifiers:** We expected our top candidates to include genes that
373 function in pathways or processes related to *Sirt1* regulation or activity. Among the most
374 interesting candidates are those involved in NAD metabolism. We identified two genes whose
375 products are part of the NADH dehydrogenase component of Complex I in the electron transport
376 chain (*NDUFS3* and *ND-PDSW*) (FlyBase Curators 2008; Gaudet *et al.* 2011). There are also
377 two NADP kinases, enzymes involved in the generation of NADP from NAD (*CG33156* and
378 *CG6145*) (Gaudet *et al.* 2011). *DUOX*, an NADPH oxidase, passes electrons from NADPH to
379 oxygen, generating hydrogen peroxide and altering the redox balance of the cell (Gaudet *et al.*
380 2011; Anh *et al.* 2011). As *Sirt1* utilizes NAD as a cofactor during its enzymatic reaction, altering
381 the balance of NAD in the cell through differential regulation of these enzymes could further
382 impact the activity of other pathways that require NAD as an electron carrier, or exacerbate the
383 phenotypes associated with *Sirt1* loss-of function (Nogueiras *et al.* 2012). We also identified two
384 genes that have previously been implicated in the regulation and/or extension of lifespan: *sugb*
385 and *CG42663* (Landis *et al.* 2003; Paik *et al.* 2012). While the role of *Sirt1* in lifespan extension
386 is still contested, the identification of other genes implicated in this process suggests shared
387 functions or pathways.

388

389 Genes involved in central glucose metabolism as well as insulin signaling are also candidate
390 modifiers. MFS5 acts as a transporter of both glucose and trehalose for the uptake of these
391 sugars from circulation (McMullen *et al.* 2021). Glucose-6-phosphatase (*G6P*) is the last rate-
392 limiting step in both gluconeogenesis and glycogenolysis, which are used to generate glucose
393 for release into the body during fasting (Gaudet *et al.* 2011; Lizák *et al.* 2019). These two genes
394 directly regulate circulating glucose levels. Candidates involved in other metabolic pathways
395 include *CTPSyn*, which encodes the rate limiting step in cytidine synthesis, the very long chain
396 fatty acid ligase *bgm*, the mannosidase *Edem2*, and the oxoglutarate dehydrogenase complex
397 subunit *CG33791* (Kang and Ryoo 2009; Gaudet *et al.* 2011; Jang *et al.* 2015; Sivachenko *et al.*
398 2016; Zhou *et al.* 2019). Partially responsible for regulating general metabolic flux through these
399 various pathways is insulin. Interestingly, a top candidate is *ilp5*, one of several insulin-like
400 peptides expressed in the insulin-producing cells (IPCs) in the *Drosophila* brain (Géminard *et al.*
401 2009). Our analysis also identified *IA-2*, a phosphatase involved in ilp secretion, *CG4168*, an
402 uncharacterized gene whose closest human orthologue *IGFALS* encodes a protein that binds to
403 and stabilizes IGF proteins in circulation, and *wrd*, a subunit in the protein phosphatase PP2A
404 that negatively regulates insulin and TOR signaling (Boisclair *et al.* 1996; Kim *et al.* 2008; Hahn
405 *et al.* 2010).

406
407 Other potential modifiers of insulin stability and signaling in circulation are *dally*, *cow*, and *Hs3st-*
408 *A*. Both *dally* and *cow* encode heparin sulfate proteoglycans, while *Hs3st-A* encodes an O-
409 sulfotransferase that acts on these proteoglycans (Filmus and Selleck 2001; Gaudet *et al.* 2011;
410 Chang and Sun 2014). Previous work has demonstrated an impact of the enzyme heparanase,
411 which cleaves heparan sulfate, on diabetic autoimmunity and complications such as
412 nephropathy (Rabelink *et al.* 2017). While this is more peripheral to the central insulin signaling
413 pathway in *Drosophila*, it highlights the utility of such factors in altering disease processes in
414 subtle ways.

415
416 Another interesting group of candidates are those associated with neuronal development and
417 function. Several members of the defective proboscis extension response (*dpr*) family were
418 represented in our list (*dpr2*, *dpr6*, and *dpr13*) along with the dpr-interacting protein *DIP-eta*.
419 The *dpr* gene family is collectively associated with synapse organization and function, as are the
420 candidate genes *fife*, *CG32373*, and *atilla* (FlyBase Curators *et al.* 2004; Kurusu *et al.* 2008;
421 Carrillo *et al.* 2015; Bruckner *et al.* 2017). We also noted candidates involved in neuropeptide
422 signaling (*rk* and *RYa-R*), voltage-gated potassium channels and their regulation (*CG5888* and
423 *CG1688*), and axon guidance (*tutl*, *CadN2*, *CG34353*, and *sbb*) (Rao *et al.* 2000; Luo *et al.*
424 2005; Prakash *et al.* 2005; Al-Anzi and Wyman 2009; Ida *et al.* 2011; Gaudet *et al.* 2011). The
425 IPCs in *Drosophila* are actually neuroendocrine cells located in the brain, as are the AKH-
426 producing cells responsible for secreting the glucagon-like hormone AKH (Géminard *et al.*
427 2006). The secretion of insulin is therefore dependent upon the correct development,
428 connection, and signaling of neuronal cells.

429
430 The immune response is another generally enriched category of modifier genes. Several
431 members of the nimrod family of immunoglobulins (*NimB2*, *NimC1*, and *NimC3*) were identified
432 by GWA. All are implicated in the innate immune response, with *NimC1* and *NimC3* in particular
433 having roles in phagocytosis (Somogyi *et al.* 2010). In response to insecticides, *LRR* regulates
434 the immune response through NF-kappaB, whose activation is an early protective event in the
435 progression and pathology of diabetes (Prisco *et al.* 2013; Irvin *et al.* 2018). Two lysozyme
436 enzymes with links to bacterial defense (*LysX* and *CG7798*) highlight the role of oxidative stress
437 and redox homeostasis in the innate immune response (FlyBase Curators 2008). As Sirt1 has
438 roles in regulating the response to oxidative stress, we looked for other genes with similar
439 functions (Brunet *et al.* 2004). As described above, *DUOX* plays a part in regulating redox
440 homeostasis through the production of hydrogen peroxide (Anh *et al.* 2011). *CG42331* encodes

441 a peroxidase that appears to be strongly enriched in the pupal fat body, and *cyp28a5* encodes
442 an oxidoreductase that, similar to LRR, is involved in the response to insecticides (FlyBase
443 Curators *et al.* 2004; Graveley *et al.* 2011; Gaudet *et al.* 2011). It is now believed that Type I
444 and Type II diabetics both suffer at least to some degree from autoimmunity (Candia *et al.*
445 2019). Exploring the direct and indirect connections of *Sirt1* to the immune response and
446 oxidative stress directly is an interesting avenue for future direction.

447

448 **Physical Interaction Network:** We generated a network of physical interactions among the 161
449 candidate genes identified above. These were identified and visualized using Cytoscape
450 software with the GeneMania plugin (Shannon *et al.* 2003; Montojo *et al.* 2010). The products of
451 37/161 candidate genes were found to physically interact with at least one other candidate gene
452 product with no more than one bridging node represented by a non-candidate gene (Figure 3A).
453 This high degree of interaction suggests that the modifiers identified in this screen are indeed
454 functioning through shared processes.

455

456 Focusing then on the 37 genes involved in physical interactions, we identified several broad
457 functional categories that could influence glucose homeostasis in the fly. The most obvious
458 category are enzymes that catalyze steps in basic metabolic pathways (N = 7). This includes
459 the NAD kinases (*CG6145* and *CG33156*) and one NADH dehydrogenase (*ND-PDSW*)
460 discussed above (Gaudet *et al.* 2011). Other metabolic candidate modifiers include *MFS3* and
461 *CTPsyn*, the rate limiting enzyme in the production of the nucleotide Cytidine triphosphate (Zhou
462 *et al.* 2019). Both of these enzymes function in pathways critically dependent upon or feeding
463 into central carbon metabolism, and their inclusion as candidate modifiers of hyperglycemia
464 supports a role for those secondary metabolic pathways as a sink for increased circulating
465 glucose. *Mtmr6* encodes a phosphatidylinositol phosphatase, a key enzyme in several signaling
466 pathways, including insulin signaling (Gaudet *et al.* 2011). Also interesting is the gene *LRP1*,

467 which is orthologous to human LDL receptor related protein 1. In addition to its role in lipid
468 homeostasis, *LRP1* has also been implicated in Alzheimer's disease, for which metabolic
469 disease and obesity are risk factors (Kang *et al.* 2000; Anstey *et al.* 2011).

470

471 Curiously, several of the genes highlighted in this analysis also happen to localize specifically to
472 the mitochondria (N = 4). *Roe1* and *porin* are both transporters involved in the import of
473 molecules into the mitochondria (Komarov *et al.* 2004; Jana Alonso *et al.* 2005; FlyBase
474 Curators 2008; Gaudet *et al.* 2011). The NADH dehydrogenases *ND-PDSW* and *NDUFS3* both
475 function in the mitochondria as well as part of Complex I in the electron transport chain
476 (Jana Alonso *et al.* 2005). Closer examination of the top GWA candidates reveals additional
477 mitochondrial localization candidates including the amino acyl tRNA synthetase *GlyRS*, the
478 membrane bound regulator of protein kinase A (*pkaap*) and the translation elongation factor
479 *mEFTu1* (Gaudet *et al.* 2011; Lu *et al.* 2016). In adult metabolic homeostasis, central carbon
480 metabolism is generally used to fuel the electron transport chain in the mitochondria and
481 generate ATP for the cell (Barry and Thummel 2016). Altering the activity of this essential
482 downstream pathway could have a clear impact on glucose utilization and disease progression
483 in diabetes.

484

485 Similar to our examination of top candidates, our physical interaction map highlighted the
486 immune response (*NimC1*, *NimC3*, *NimB2*, and *LRR*) and neuronal function. *Tut1*, *dpr2*, and
487 *DIP-eta*, and *wb* are all involved in synapse organization and axon guidance, while *Pax* and
488 *rhea* are involved in focal adhesion (Delon and Brown 2009). The identification of genes
489 important for cellular communication suggests that some of the modifiers identified in this study
490 have roles in tissues other than the fat body, such as the IPC and APC neurons. This is an
491 important avenue of future exploration.

492

493 **Gene Set Enrichment Analysis (GSEA):** In the second approach, we performed GSEA
494 analysis to identify gene ontology terms for which associated variants are enriched. Unlike
495 traditional GO analysis, which relies upon a set of genes based on a P-value cutoff, GSEA
496 examines the entire gene set (Dyer *et al.* 2008). For each defined GO category, GSEA
497 determines whether the members of that category are randomly distributed throughout the
498 ranked gene list provided or if they are enriched for the lower p-values found at the top of that
499 list. GO categories enriched at the top of the list describe important functions of the gene set.
500 GSEA identified 52 significantly associated gene sets (≥ 3 genes) with positive enrichment
501 scores at a p-value of <0.05 (Table S6, Figure 3B). The top two gene sets implicate neuronal
502 function and communication in the *Sirt1i*-associated hyperglycemia phenotype: calcium-
503 activated potassium channel activity (GO:0015269, $P = 1.1E-3$) and maintenance of presynaptic
504 active zone structure (GO:0048790, $P = 1.2E-3$). Similar categories can be found through the
505 list of significantly associated gene sets, including dendrite morphogenesis (GO:0048813, $P =$
506 0.049), which represents the largest group of genes at $N = 119$ and contains two of the top
507 GWA candidates (*slit* and *fruitless*). Coupled with the neuronal genes identified in our physical
508 interaction network, this suggests that function in the neuroendocrine cells could play a big role
509 in glucose homeostasis in the fat body.

510

511 Also enriched are taste receptor activity (GO:0008527, $P = 0.013$) and sensory reception of
512 taste (GO:0050909, $P = 0.018$). These categories highlight a yet unconsidered factor that must
513 be taken into account with metabolic phenotypes: that of feeding and diet. While all flies were
514 collected under identical conditions and were maintained on the same diet, it is nonetheless
515 possible that some may simply be eating more due to differences in the sensing of satiation or
516 to differences in perception of taste. These differences in perception and consumption can have
517 detectable impacts on metabolic phenotypes (May *et al.* 2019).

518

519 As expected, we also see evidence of general metabolic processes. Some, like alpha,alpha-
520 trehalase activity (GO:0004555, P = 0.043) and phosphatidylinositol transporter activity
521 (GO:0008526, P = 0.013) have direct links to glucose metabolism and insulin signaling. Others,
522 such as oxysterol binding (GO:0008142, P = 0.026), glutamate biosynthetic process
523 (GO:0006537, P = 0.043), and isoprenoid biosynthetic process (GO:0008299, P = 0.048)
524 function more peripherally to carbon metabolism and are likely influencing hyperglycemia by
525 their general contribution to physiological homeostasis.

526

527 Another interesting group of GO categories highlighted by GSEA are RNA processing functions.
528 rRNA (uridine-2'-O-)-methyltransferase activity (GO:0008650, P = 2.4E-3) is the fourth most
529 associated category as ranked by p-value, and others such as snoRNA binding (GO:0030515, P
530 = 0.014) reiterating this function. The presence of RNA processing categories is of particular
531 interest because three of the top candidate genes by GWA are splicing factors (*bru1*, *fand*, and
532 *snRNP-U1-70k*) (Park *et al.* 2004; Oas *et al.* 2014; Spletter *et al.* 2015). While it is unclear how
533 rRNA or mRNA processing may directly or indirectly influence glucose homeostasis in
534 particular, the identification of this process through several different methods of analysis is
535 striking and worth further exploration.

536

537 *Functional analysis of candidate modifier genes*

538 To confirm the roles of our candidate genes in regulating glucose homeostasis, we elected to
539 test the impact of loss of modifier expression for 16 of the most significant candidates for which
540 we were able to obtain transgenic RNAi lines (Table 1). We crossed the RNAi strains targeting
541 each of these modifiers into the *R4>Sirt1i* line, aged the resulting progeny for 2-3 weeks, and
542 measured glucose in fasted males. We also measured protein levels as a control. Knockdown of
543 modifier genes did not significantly alter protein levels as compared to a genetically matched
544 control (Figure S7). Knockdown of the genes *CG4168*, *CG5888*, and *uif* resulted in suppression

545 of the hyperglycemia phenotype, with a significant decrease in glucose content per fly compared
546 to controls expressing *R4>Sirt1i* (Figure 4). These results demonstrate that many of the top
547 GWA candidate modifiers are capable of modifying the hyperglycemia phenotypes associated
548 with the *R4>Sirt1i* model of diabetes.

549

550

DISCUSSION

551 Identifying and characterizing the genetic factors influencing the severity of diabetes is critical to
552 early diagnosis. Prevention is still the best strategy available, and providing patients at high risk
553 for complications with knowledge of that risk could prevent the worst symptoms from
554 manifesting. It could even enable intervention before the progression of disease is irreversible.

555

556 In this study, we identified and analyzed a number of candidate modifiers of hyperglycemia in a
557 previously characterized model of diabetes, *Sirt1* loss-of-function. We used the DGRP as an
558 unbiased source of natural genetic variation for this screen. This is the first time a genetic model
559 of metabolic dysfunction has been put to this use, as previous screens have either focused on
560 dietary stress as a source of metabolic disease or on the impact of genotype on metabolic
561 parameters under non-stressed conditions (Mackay *et al.* 2012; Ivanov *et al.* 2015; Nelson *et al.*
562 2016; Jehrke *et al.* 2018; Everman *et al.* 2019). We observed very little overlap in modifier
563 candidates between our observations and these studies. This is consistent with previous work
564 demonstrating that even when the observed phenotypes are similar or nearly identical, the
565 overlap in modifiers is often small in different models of disease (Palu *et al.* 2019). One
566 exception is a screen for the response to starvation resistance performed by Everman *et al.* in
567 2018. They identified *CG15803*, a transporter of unknown function that was also identified in our
568 studies (Everman and Morgan 2018). While our preliminary analysis suggests that this gene
569 does not function in the fat body, it is possible that it could have a role in another physiologically
570 relevant tissue such as the IPCs or APCs. Indeed, *CG15803* appears to be most highly

571 expressed in the head and CNS (Graveley *et al.* 2011). This is an interesting avenue of future
572 exploration.

573
574 We did observe overlap in general gene categories with previous studies, even when direct
575 overlaps were few. This was found to be true for modifiers of neuronal function. In a broad
576 exploration of genetic variation in the nutrient response that looked at triglycerides, starvation
577 resistance, mass, and glucose, *NimB3* was identified as a candidate modifier (Nelson *et al.*
578 2016). While *NimB3* was not identified in this screen, we did find *NimB2*, *NimC1*, and *NimC3*.
579 *Fife*, which also has roles in synapse organization, was identified in this study and one for
580 starvation resistance (Mackay *et al.* 2012). As mentioned above, both the IPCs and APCs are
581 neuroendocrine cells found in or near the brain (Géminard *et al.* 2006). Maintenance of neuronal
582 function would be critical to hormonal balance as a result. Furthermore, it is broadly
583 acknowledged that metabolic homeostasis is also dependent upon feeding rate, over which the
584 central nervous system has some sway (Owusu-Ansah and Perrimon 2014). The identification
585 of neuronal genes in each analysis suggests that regulation of particular neuronal pathways and
586 cells is critical to the maintenance of physiological homeostasis.

587
588 Given the prevalence of neuronal and sensory perception genes in the analysis, a concern
589 could be raised for the role feeding rate could be playing in the variation of glucose across the
590 DGRP. To assess this, we compared glucose with male feeding rate in a previous analysis
591 (Table S3) (Garlapow *et al.* 2015). We saw no correlation whatsoever, indicating that while
592 nutrient sensing may play a role in the response to Sirt1i-induced hyperglycemia, it is not the
593 driving factor in the variation observed in this screen (Figure S8).

594
595 Another interesting category highlighted through several analysis methods is the innate immune
596 response. While it has long been known that Type I diabetes is an autoimmune disorder, it has

597 recently been acknowledged that Type II diabetics also display symptoms of autoimmunity
598 (Candia *et al.* 2019). Furthermore, insulin resistance has frequently been associated with
599 inflammation, and the presence of macrophages in the adipose tissue is a hallmark of obesity
600 and diabetes (Wu and Ballantyne 2020). Modifiers associated with innate immunity serve
601 therefore as validation to the study as a whole, and examination of these genes and their
602 function in the context of the *Sirt1* loss-of-function model will be an intriguing focus of future
603 research.

604
605 An important component of this study is the validation of top candidate modifiers using RNAi-
606 mediated knockdown of gene expression. We obtained strains expression transgenic RNAi
607 constructs targeting 16 of the most significant candidates (Table 1). We found that reduced
608 expression of three candidates specifically in the fat body resulted in significant suppression of
609 hyperglycemia: *CG4168*, *CG5888*, and *uif* (Figure 4). We also noted a consistent, though not
610 significant, decrease in glucose for two independent RNAi constructs targeting *CTPSyn*,
611 suggesting that this gene warrants further study (Figure 4, data not shown). The remainder of
612 the genes had no significant or consistent impact on hyperglycemia in the model of *Sirt1* loss-of-
613 function (Figure 4). There were no enhancing modifiers: loss of modifier expression did not lead
614 to increased glucose levels for any of the tested genes. This could be because hyperglycemia is
615 already quite strong in the *Sirt1* loss-of-function model, or because we simply did not hit on any
616 enhancing modifiers. Of greater concern is the lack of any response for 13 of the 16 tested
617 candidates. One explanation may be found in the large number of known neuronal genes
618 identified in this analysis. This modifier RNAi screen specifically focused on the expression of
619 the RNAi against the candidate genes in the fat body, where expression of *Sirt1* is also reduced.
620 If, however, the function of a modifier gene is primarily concentrated in the IPCs, as with *ilp5*,
621 reducing its expression in the fat body would have little effect on the disease phenotypes in

622 question. We will examine the role of modifier genes not only in the fat body but in the IPCs,
623 APCs, and other physiologically relevant tissues in future work.

624

625 Of immediate interest is of course the mechanism of action for the three suppressor genes that
626 were confirmed by RNAi in the fat body. Of these, *CG5888* is also the top GWA candidate ($P =$
627 $2.80E-07$). While largely uncharacterized, *CG5888* has been identified as a component or
628 activator of voltage-gated potassium channels by sequence homology (Gaudet *et al.* 2011).
629 Intriguingly, it has also been implicated JNK signaling by a previous RNAi screen (Bond and
630 Foley 2009). JNK signaling is commonly activated by cellular stress and can activate apoptosis.
631 It also has important roles in the signaling pathways commonly used by the immune system
632 (Bond and Foley 2009; Shlevkov and Morata 2012). A potential role for *CG5888* in immune
633 pathways has yet to be explored and could be an exciting area of further discovery.

634

635 *Uninflatable (uif)* encodes a single pass transmembrane protein found on the apical membrane
636 of epithelial cells and has been found to enable Notch signaling (Loubéry *et al.* 2014). It has
637 also been found to exacerbate disease in a *Drosophila* model of muscular dystrophy
638 (Kucherenko *et al.* 2011), and its closest human orthologue ELAPOR1 is a regulator of
639 apoptosis and autophagy (Deng *et al.* 2010). Both of these processes are commonly disrupted
640 through inappropriate activation in metabolic disease, and might provide some explanation for
641 the impact of *uif* on *Sirt1i*-associated phenotypes (Bugliani *et al.* 2019).

642

643 Perhaps the most intriguing finding is *CG4168* as the modifier with the strongest impact on
644 *Sirt1i*-associated hyperglycemia. The protein encoded by *CG4168* is of unknown function, but
645 its closest human orthologue (*IGFALS*) encodes a serum protein that binds to insulin-like growth
646 factors (IGF) in circulation (Boisclair *et al.* 1996). In mammals, association with IGFALS
647 increases the half-life of insulin-like growth factors in the serum as well as their retention in

648 circulation. While studies of IGFALS in mammals has not shown a role for it in regulating insulin
649 signaling, the *Drosophila* ilp peptides are used for both IGF and insulin signaling activation
650 (Géminard *et al.* 2006). It is possible that secretion of the factor encoded by *CG4168* from the
651 fat body could increase ilp retention in circulation, whereas its loss could result in faster
652 clearance of ilps from circulation. Under conditions that promote insulin resistance, such as the
653 loss of *Sirt1*, it is possible that reduced ilp levels in the hemolymph could slow or prevent insulin
654 resistance and hyperglycemia. Further exploration of the mechanisms behind the action of
655 *CG4168* could reveal important insights into circulating insulin-binding factors and their role in
656 diabetes.

657

658 In conclusion, we have identified a number of pathways and processes involved in the degree of
659 hyperglycemia in a genetic model of diabetes. Examination of the candidate genes and
660 pathways described above in this model as well as other models of metabolic dysfunction will
661 shed new light on the mechanism by which insulin resistance and related complications disease
662 onset, progression, and severity. Furthermore, the candidates identified as suppressors could
663 serve as promising targets for therapeutics in diabetes and related metabolic disorders.

664

665 **DATA AVAILABILITY STATEMENT**

666 Strains and stocks are available upon request, as is code for GSEA. Genomic sequence for the
667 DGRP is available at <http://dgrp.gnets.ncsu.edu/>. Supplemental material is available at FigShare
668 (<https://figshare.com/s/2b0b0237de0f94139a4f>).

669

670 **ACKNOWLEDGEMENTS**

671 We thank Clement Y. Chow for contributions to the data analysis in this project, as well as
672 reagents and comments. This research was supported by a Faculty Summer Research Grant
673 through the Purdue University-Fort Wayne Office of Sponsored Projects to RASP as well as the

674 Purdue University-Fort Wayne Department of Biology. KGO is supported by the NIGMS
675 Genetics T32 Fellowship from the University of Utah (T32GM007464).

676

677

REFERENCES

678 Al-Anzi B., and R. J. Wyman, 2009 The *Drosophila* immunoglobulin gene turtle encodes
679 guidance molecules involved in axon pathfinding. *Neural Dev.* 2009 41 4: 1–15.

680 <https://doi.org/10.1186/1749-8104-4-31>

681 Anh N. T. T., M. Nishitani, S. Harada, M. Yamaguchi, and K. Kamei, 2011 Essential Role of
682 Duox in Stabilization of *Drosophila* Wing. *J. Biol. Chem.* 286: 33244–33251.

683 <https://doi.org/10.1074/JBC.M111.263178>

684 Anstey K. J., N. Cherbuin, M. Budge, and J. Young, 2011 Body mass index in midlife and late-
685 life as a risk factor for dementia: a meta-analysis of prospective studies. *Obes. Rev.* 12:

686 e426–e437. <https://doi.org/10.1111/J.1467-789X.2010.00825.X>

687 Arrese E. L., and J. L. Soulages, 2010 Insect Fat Body: Energy, Metabolism, and Regulation.

688 *Annu. Rev. Entomol.* 55: 207–225. <https://doi.org/10.1146/annurev-ento-112408-085356>

689 Barroso I., and M. I. McCarthy, 2019 The Genetic Basis of Metabolic Disease. *Cell* 177: 146–
690 161. <https://doi.org/10.1016/j.cell.2019.02.024>

691 Barry W. E., and C. S. Thummel, 2016 The *Drosophila* HNF4 nuclear receptor promotes
692 glucose-stimulated insulin secretion and mitochondrial function in adults. *Elife* 5.

693 <https://doi.org/10.7554/ELIFE.11183>

694 Beebe K., M. M. Robins, E. J. Hernandez, G. Lam, M. A. Horner, *et al.*, 2020 *Drosophila*
695 estrogen-related receptor directs a transcriptional switch that supports adult glycolysis and

696 lipogenesis. *Genes Dev.* 34: 701. <https://doi.org/10.1101/GAD.335281.119>

697 Biason-Lauber A., M. Böni-Schnetzler, B. P. Hubbard, K. Bouzakri, A. Brunner, *et al.*, 2013

698 Identification of a SIRT1 Mutation in a Family with Type 1 Diabetes. *Cell Metab.* 17: 448–

699 455. <https://doi.org/10.1016/J.CMET.2013.02.001>

- 700 Boisclair Y. R., D. Seto, S. Hsieh, K. R. Hurst, and G. T. Ooi, 1996 Organization and
701 chromosomal localization of the gene encoding the mouse acid labile subunit of the insulin-
702 like growth factor binding complex. *Proc. Natl. Acad. Sci.* 93: 10028–10033.
703 <https://doi.org/10.1073/PNAS.93.19.10028>
- 704 Bond D., and E. Foley, 2009 A quantitative RNAi screen for JNK modifiers identifies Pvr as a
705 novel regulator of *Drosophila* immune signaling. *PLoS Pathog.* 5.
706 <https://doi.org/10.1371/JOURNAL.PPAT.1000655>
- 707 Botden I. P. G., M. C. Zillikens, S. R. de Rooij, J. G. Langendonk, A. H. J. Danser, *et al.*, 2012
708 Variants in the SIRT1 Gene May Affect Diabetes Risk in Interaction With Prenatal
709 Exposure to Famine. *Diabetes Care* 35: 424–426. <https://doi.org/10.2337/DC11-1203>
- 710 Boutant M., and C. Cantó, 2014 SIRT1 metabolic actions: Integrating recent advances from
711 mouse models. *Mol. Metab.* 3: 5–18.
- 712 Bruckner J. J., H. Zhan, S. J. Gratz, M. Rao, F. Ukken, *et al.*, 2017 Fife organizes synaptic
713 vesicles and calcium channels for high-probability neurotransmitter release. *J. Cell Biol.*
714 216: 231–246. <https://doi.org/10.1083/JCB.201601098>
- 715 Brunet A., L. Sweeney, J. Sturgill, K. Chua, P. Greer, *et al.*, 2004 Stress-dependent regulation
716 of FOXO transcription factors by the SIRT1 deacetylase. *Science* 303: 2011–2015.
717 <https://doi.org/10.1126/SCIENCE.1094637>
- 718 Bugliani M., S. Mossuto, F. Grano, M. Suleiman, L. Marselli, *et al.*, 2019 Modulation of
719 Autophagy Influences the Function and Survival of Human Pancreatic Beta Cells Under
720 Endoplasmic Reticulum Stress Conditions and in Type 2 Diabetes. *Front. Endocrinol.*
721 (Lausanne). 10: 52. <https://doi.org/10.3389/fendo.2019.00052>
- 722 Cabrera A. P., R. N. Mankad, L. Marek, R. Das, S. Rangasamy, *et al.*, 2020 Genotypes and
723 Phenotypes: A Search for Influential Genes in Diabetic Retinopathy. *Int. J. Mol. Sci.* 2020,
724 Vol. 21, Page 2712 21: 2712. <https://doi.org/10.3390/IJMS21082712>
- 725 Candia P. de, F. Prattichizzo, S. Garavelli, V. De Rosa, M. Galgani, *et al.*, 2019 Type 2

- 726 Diabetes: How Much of an Autoimmune Disease? *Front. Endocrinol. (Lausanne)*. 10: 451.
727 <https://doi.org/10.3389/FENDO.2019.00451>
- 728 Carrillo R. A., E. Özkan, K. P. Menon, S. Nagarkar-Jaiswal, P.-T. Lee, *et al.*, 2015 Control of
729 Synaptic Connectivity by a Network of *Drosophila* IgSF Cell Surface Proteins. *Cell* 163:
730 1770–1782. <https://doi.org/10.1016/J.CELL.2015.11.022>
- 731 CDC, 2020 National Diabetes Statistics Report 2020. Estimates of diabetes and its burden in
732 the United States.
- 733 Chang Y.-H., and Y. H. Sun, 2014 Carrier of Wingless (Cow), a Secreted Heparan Sulfate
734 Proteoglycan, Promotes Extracellular Transport of Wingless. *PLoS One* 9: e111573.
735 <https://doi.org/10.1371/JOURNAL.PONE.0111573>
- 736 Chow C. Y., M. F. Wolfner, and A. G. Clark, 2013 Using natural variation in *Drosophila* to
737 discover previously unknown endoplasmic reticulum stress genes. *Proc Natl Acad Sci U S*
738 *A* 110: 9013–9018. <https://doi.org/10.1073/pnas.1307125110>
- 739 Chow C. Y., F. W. Avila, A. G. Clark, and M. F. Wolfner, 2015 Induction of excessive
740 Endoplasmic reticulum stress in the *Drosophila* male accessory gland results in infertility.
741 *PLoS One* 10: 1–12. <https://doi.org/10.1371/journal.pone.0119386>
- 742 Chow C. Y., 2016 Bringing genetic background into focus. *Nat. Rev. Genet.* 17: 63–64.
743 <https://doi.org/10.1038/nrg.2015.9>
- 744 Chow C. Y., K. J. P. Kelsey, M. F. Wolfner, and A. G. Clark, 2016 Candidate genetic modifiers
745 of retinitis pigmentosa identified by exploiting natural variation in *Drosophila*. *Hum. Mol.*
746 *Genet.* 25: 651–659. <https://doi.org/10.1093/HMG/DDV502>
- 747 Chow C. Y., and L. T. Reiter, 2017 Etiology of Human Genetic Disease on the Fly. *Trends*
748 *Genet.* 33: 391–398. <https://doi.org/10.1016/j.tig.2017.03.007>
- 749 Delon I., and N. H. Brown, 2009 The integrin adhesion complex changes its composition and
750 function during morphogenesis of an epithelium. *J. Cell Sci.* 122: 4363–4374.
751 <https://doi.org/10.1242/JCS.055996>

- 752 Deng L., J. Feng, and R. R. Broaddus, 2010 The novel estrogen-induced gene EIG121
753 regulates autophagy and promotes cell survival under stress. *Cell Death Dis.* 1: e32.
754 <https://doi.org/10.1038/CDDIS.2010.9>
- 755 DiAngelo J. R., and M. J. Birnbaum, 2009 Regulation of Fat Cell Mass by Insulin in *Drosophila*
756 *melanogaster*. *Mol. Cell. Biol.* 29: 6341–6352. <https://doi.org/10.1128/mcb.00675-09>
- 757 Dyer M. D., T. M. Murali, and B. W. Sobral, 2008 The Landscape of Human Proteins Interacting
758 with Viruses and Other Pathogens. *PLoS Pathog.* 4: e32.
759 <https://doi.org/10.1371/journal.ppat.0040032>
- 760 Everman E. R., and T. J. Morgan, 2018 Antagonistic pleiotropy and mutation accumulation
761 contribute to age-related decline in stress response. *Evolution (N. Y.)*. 72: 303–317.
762 <https://doi.org/10.1111/EVO.13408>
- 763 Everman E. R., C. L. McNeil, J. L. Hackett, C. L. Bain, and S. J. Macdonald, 2019 Dissection of
764 Complex, Fitness-Related Traits in Multiple *Drosophila* Mapping Populations Offers Insight
765 into the Genetic Control of Stress Resistance. *Genetics* 211: 1449–1467.
766 <https://doi.org/10.1534/genetics.119.301930>
- 767 Filmus J., and S. B. Selleck, 2001 Glypicans: proteoglycans with a surprise. *J. Clin. Invest.* 108:
768 497–501. <https://doi.org/10.1172/JCI13712>
- 769 Flegal K., D. Kruszon-Moran, M. Carroll, C. Fryar, and C. Ogden, 2016 Trends in Obesity
770 Among Adults in the United States, 2005 to 2014. *JAMA* 315: 2284–2291.
771 <https://doi.org/10.1001/JAMA.2016.6458>
- 772 FlyBase Curators, Swiss-Prot Project Members, and InterPro Project Members, 2004 Gene
773 Ontology annotation in FlyBase through association of InterPro records with GO terms.
- 774 FlyBase Curators, 2008 Assigning Gene Ontology (GO) terms by sequence similarity in
775 FlyBase.
- 776 Garlapow M. E., W. Huang, M. T. Yarboro, K. R. Peterson, and T. F. C. Mackay, 2015
777 Quantitative Genetics of Food Intake in *Drosophila melanogaster*. *PLoS One* 10:

778 e0138129. <https://doi.org/10.1371/JOURNAL.PONE.0138129>

779 Gaudet P., M. S. Livstone, S. E. Lewis, and P. D. Thomas, 2011 Phylogenetic-based
780 propagation of functional annotations within the Gene Ontology consortium. *Brief.*
781 *Bioinform.* 12: 449–462. <https://doi.org/10.1093/bib/bbr042>

782 Géminard C., N. Arquier, S. Layalle, M. Bourouis, M. Slaidina, *et al.*, 2006 Control of
783 metabolism and growth through insulin-like peptides in *Drosophila*. *Diabetes* 55: S5–S8.
784 <https://doi.org/10.2337/db06-S001>

785 Géminard C., E. J. Rulifson, and P. Léopold, 2009 Remote Control of Insulin Secretion by Fat
786 Cells in *Drosophila*. *Cell Metab.* 10: 199–207. <https://doi.org/10.1016/j.cmet.2009.08.002>

787 Graveley B. R., G. May, A. N. Brooks, J. W. Carlson, L. Cherbas, *et al.*, 2011 The *D.*
788 *melanogaster* transcriptome: modENCODE RNA-Seq data for dissected tissues

789 Hahn K., M. Miranda, V. A. Francis, J. Vendrell, A. Zorzano, *et al.*, 2010 PP2A Regulatory
790 Subunit PP2A-B' Counteracts S6K Phosphorylation. *Cell Metab.* 11: 438–444.
791 <https://doi.org/10.1016/J.CMET.2010.03.015>

792 He B. Z., M. Z. Ludwig, D. A. Dickerson, L. Barse, B. Arun, *et al.*, 2014 Effect of Genetic
793 Variation in a *Drosophila* Model of Diabetes-Associated Misfolded Human Proinsulin.
794 *Genetics* 196: 557. <https://doi.org/10.1534/GENETICS.113.157800>

795 Huang W., A. Massouras, Y. Inoue, J. Peiffer, M. Ràmia, *et al.*, 2014 Natural variation in
796 genome architecture among 205 *Drosophila melanogaster* Genetic Reference Panel lines.
797 *Genome Res.* 24: 1193–208. <https://doi.org/10.1101/gr.171546.113>

798 Ida T., T. Takahashi, H. Tominaga, T. Sato, K. Kume, *et al.*, 2011 Identification of the novel
799 bioactive peptides dRYamide-1 and dRYamide-2, ligands for a neuropeptide Y-like
800 receptor in *Drosophila*. *Biochem. Biophys. Res. Commun.* 410: 872–877.
801 <https://doi.org/10.1016/J.BBRC.2011.06.081>

802 Irvin A. E., G. Jhala, Y. Zhao, T. S. Blackwell, B. Krishnamurthy, *et al.*, 2018 NF- κ B is weakly
803 activated in the NOD mouse model of type 1 diabetes. *Sci. Reports* 2018 8: 1–7.

- 804 <https://doi.org/10.1038/s41598-018-22738-3>
- 805 Ivanov D. K., V. Escott-Price, M. Ziehm, M. M. Magwire, T. F. C. Mackay, *et al.*, 2015 Longevity
806 GWAS using the drosophila genetic reference panel. *Journals Gerontol. - Ser. A Biol. Sci.*
807 *Med. Sci.* 70: 1470–1478. <https://doi.org/10.1093/gerona/glv047>
- 808 Ivy J., A. Klar, and J. Hicks, 1986 Cloning and characterization of four SIR genes of
809 *Saccharomyces cerevisiae*. *Mol. Cell. Biol.* 6: 688–702.
810 <https://doi.org/10.1128/MCB.6.2.688-702.1986>
- 811 Jana Alonso, Javier M. Rodriguez, and Luis Alberto Baena-López, and J. F. Santarén*, 2005
812 Characterization of the *Drosophila melanogaster* Mitochondrial Proteome. *J. Proteome*
813 *Res.* 4: 1636–1645. <https://doi.org/10.1021/PR050130C>
- 814 Jang B.-Y., H. D. Ryoo, J. Son, K.-C. Choi, D.-M. Shin, *et al.*, 2015 Role of *Drosophila* EDEMs
815 in the degradation of the alpha-1-antitrypsin Z variant. *Int. J. Mol. Med.* 35: 870–876.
816 <https://doi.org/10.3892/IJMM.2015.2109>
- 817 Jehrke L., F. A. Stewart, A. Droste, and M. Beller, 2018 The impact of genome variation and diet
818 on the metabolic phenotype and microbiome composition of *Drosophila melanogaster*. *Sci.*
819 *Rep.* 8. <https://doi.org/10.1038/S41598-018-24542-5>
- 820 Kang D. E., C. U. Pietrzik, L. Baum, N. Chevallier, D. E. Merriam, *et al.*, 2000 Modulation of
821 amyloid β -protein clearance and Alzheimer's disease susceptibility by the LDL receptor–
822 related protein pathway. *J. Clin. Invest.* 106: 1159–1166. <https://doi.org/10.1172/JCI11013>
- 823 Kang M.-J., and H. D. Ryoo, 2009 Suppression of retinal degeneration in *Drosophila* by
824 stimulation of ER-associated degradation. *Proc. Natl. Acad. Sci. U. S. A.* 106: 17043–8.
825 <https://doi.org/10.1073/pnas.0905566106>
- 826 Kim J., H. Bang, S. Ko, I. Jung, H. Hong, *et al.*, 2008 *Drosophila* *ia2* modulates secretion of
827 insulin-like peptide. *Comp. Biochem. Physiol. Part A Mol. Integr. Physiol.* 151: 180–184.
828 <https://doi.org/10.1016/J.CBPA.2008.06.020>
- 829 Komarov A. G., B. H. Graham, W. J. Craigen, and M. Colombini, 2004 The Physiological

- 830 Properties of a Novel Family of VDAC-Like Proteins from *Drosophila melanogaster*.
831 *Biophys. J.* 86: 152–162. [https://doi.org/10.1016/S0006-3495\(04\)74093-X](https://doi.org/10.1016/S0006-3495(04)74093-X)
- 832 Kucherenko M. M., A. K. Marrone, V. M. Rishko, H. de F. Magliarelli, and H. R. Shcherbata,
833 2011 Stress and muscular dystrophy: A genetic screen for Dystroglycan and Dystrophin
834 interactors in *Drosophila* identifies cellular stress response components. *Dev. Biol.* 352:
835 228–242. <https://doi.org/10.1016/J.YDBIO.2011.01.013>
- 836 Kurusu M., A. Cording, M. Taniguchi, K. Menon, E. Suzuki, *et al.*, 2008 A Screen of Cell-Surface
837 Molecules Identifies Leucine-Rich Repeat Proteins as Key Mediators of Synaptic Target
838 Selection. *Neuron* 59: 972–985. <https://doi.org/10.1016/J.NEURON.2008.07.037>
- 839 Landis G. N., D. Bhole, and J. Tower, 2003 A search for doxycycline-dependent mutations that
840 increase *Drosophila melanogaster* life span identifies the VhaSFD, Sugar baby, filamin, fwd
841 and Cctlgenes. *Genome Biol.* 2003 42 4: 1–14. <https://doi.org/10.1186/GB-2003-4-2-R8>
- 842 Lavoy S., V. G. Chittoor-Vinod, C. Y. Chow, and I. Martin, 2018 Genetic Modifiers of
843 Neurodegeneration in a *Drosophila* Model of Parkinson’s Disease. *Genetics* 209: 1345–
844 1356. <https://doi.org/10.1534/genetics.118.301119>
- 845 Lee G., and J. H. Park, 2004 Hemolymph Sugar Homeostasis and Starvation-Induced
846 Hyperactivity Affected by Genetic Manipulations of the Adipokinetic Hormone-Encoding
847 Gene in *Drosophila melanogaster*. *Genetics* 167: 311–323.
848 <https://doi.org/10.1534/GENETICS.167.1.311>
- 849 Li X., S. Zhang, G. Blander, J. Tse, M. Krieger, *et al.*, 2007 SIRT1 deacetylates and positively
850 regulates the nuclear receptor LXR. *Mol. Cell* 28: 91–106.
851 <https://doi.org/10.1016/J.MOLCEL.2007.07.032>
- 852 Lizák B., A. Szarka, Y. Kim, K. Choi, C. E. Németh, *et al.*, 2019 Glucose Transport and
853 Transporters in the Endomembranes. *Int. J. Mol. Sci.* 20.
854 <https://doi.org/10.3390/IJMS20235898>
- 855 Loubéry S., C. Seum, A. Moraleda, A. Daeden, M. Fürthauer, *et al.*, 2014 Uninflatable and

- 856 Notch Control the Targeting of Sara Endosomes during Asymmetric Division. *Curr. Biol.* 24:
857 2142–2148. <https://doi.org/10.1016/J.CUB.2014.07.054>
- 858 Lu J., S. J. Marygold, W. H. Gharib, and B. Suter, 2016 The aminoacyl-tRNA synthetases of
859 *Drosophila melanogaster*. <https://doi.org/10.1080/19336934.2015.1101196> 9: 53–61.
860 <https://doi.org/10.1080/19336934.2015.1101196>
- 861 Luo C.-W., E. M. Dewey, S. Sudo, J. Ewer, S. Y. Hsu, *et al.*, 2005 Bursicon, the insect cuticle-
862 hardening hormone, is a heterodimeric cystine knot protein that activates G protein-
863 coupled receptor LGR2. *Proc. Natl. Acad. Sci.* 102: 2820–2825.
864 <https://doi.org/10.1073/PNAS.0409916102>
- 865 Mackay T. F. C., S. Richards, E. A. Stone, A. Barbadilla, J. F. Ayroles, *et al.*, 2012 The
866 *Drosophila melanogaster* Genetic Reference Panel. *Nature* 482: 173–178.
867 <https://doi.org/10.1038/nature10811>
- 868 May C. E., A. Vaziri, Y. Q. Lin, O. Grushko, M. Khabiri, *et al.*, 2019 High Dietary Sugar
869 Reshapes Sweet Taste to Promote Feeding Behavior in *Drosophila melanogaster*. *Cell*
870 *Rep.* 27: 1675-1685.e7. <https://doi.org/10.1016/J.CELREP.2019.04.027>
- 871 McMullen E., A. Weiler, H. M. Becker, and S. Schirmeier, 2021 Plasticity of Carbohydrate
872 Transport at the Blood-Brain Barrier. *Front. Behav. Neurosci.* 0: 271.
873 <https://doi.org/10.3389/FNBEH.2020.612430>
- 874 Millington J. W., and E. J. Rideout, 2018 Sex differences in *Drosophila* development and
875 physiology. *Curr. Opin. Physiol.* 6: 46–56. <https://doi.org/10.1016/J.COPHYS.2018.04.002>
- 876 Montojo J., K. Zuberi, H. Rodriguez, F. Kazi, G. Wright, *et al.*, 2010 GeneMANIA Cytoscape
877 plugin: fast gene function predictions on the desktop. *Bioinformatics* 26: 2927–8.
878 <https://doi.org/10.1093/bioinformatics/btq562>
- 879 Nelson C. S., J. N. Beck, K. A. Wilson, E. R. Pilcher, P. Kapahi, *et al.*, 2016 Cross-phenotype
880 association tests uncover genes mediating nutrient response in *Drosophila*. *BMC*
881 *Genomics* 17. <https://doi.org/10.1186/s12864-016-3137-9>

- 882 Nogueiras R., K. M. Habegger, N. Chaudhary, B. Finan, A. S. Banks, *et al.*, 2012 Sirtuin 1 and
883 sirtuin 3: Physiological modulators of metabolism. *Physiol. Rev.* 92: 1479–1514.
884 <https://doi.org/10.1152/physrev.00022.2011>
- 885 Oas S. T., A. L. Bryantsev, and R. M. Cripps, 2014 Arrest is a regulator of fiber-specific
886 alternative splicing in the indirect flight muscles of *Drosophila*. *J. Cell Biol.* 206: 895–908.
887 <https://doi.org/10.1083/JCB.201405058>
- 888 Owusu-Ansah E., and N. Perrimon, 2014 Modeling metabolic homeostasis and nutrient sensing
889 in *Drosophila*: implications for aging and metabolic diseases. *Dis. Model. Mech.* 7: 343–
890 350. <https://doi.org/10.1242/DMM.012989>
- 891 Paik D., Y. G. Jang, Y. E. Lee, Y. N. Lee, R. Yamamoto, *et al.*, 2012 Misexpression screen
892 delineates novel genes controlling *Drosophila* lifespan. *Mech. Ageing Dev.* 133: 234–245.
893 <https://doi.org/10.1016/J.MAD.2012.02.001>
- 894 Palu R. A. S., and C. S. Thummel, 2016 Sir2 Acts through Hepatocyte Nuclear Factor 4 to
895 maintain insulin Signaling and Metabolic Homeostasis in *Drosophila*. *PLoS Genet.* 12: 1–
896 18. <https://doi.org/10.1371/journal.pgen.1005978>
- 897 Palu R. A. S., and C. Y. Chow, 2018 Baldspot/ELOVL6 is a conserved modifier of disease and
898 the ER stress response. *PLoS Genet.* 14. <https://doi.org/10.1101/261206>
- 899 Palu R. A. S., E. Ong, K. Stevens, S. Chung, K. G. Owings, *et al.*, 2019 Natural Genetic
900 Variation Screen in *Drosophila* Identifies Wnt Signaling, Mitochondrial Metabolism, and
901 Redox Homeostasis Genes as Modifiers of Apoptosis. *G3 Genes|Genomes|Genetics* 9:
902 g3.400722.2019. <https://doi.org/10.1534/g3.119.400722>
- 903 Palu R. A. S., H. M. Dalton, and C. Y. Chow, 2020 Decoupling of Apoptosis from Activation of
904 the ER Stress Response by the *Drosophila* Metallopeptidase superdeath. *Genetics* 214:
905 913–925. <https://doi.org/10.1534/GENETICS.119.303004>
- 906 Park J. W., K. Parisky, A. M. Celotto, R. A. Reenan, and B. R. Graveley, 2004 Identification of
907 alternative splicing regulators by RNA interference in *Drosophila*. *Proc. Natl. Acad. Sci.*

908 101: 15974–15979. <https://doi.org/10.1073/PNAS.0407004101>

909 Picard F., M. Kurtev, N. Chung, A. Topark-Ngarm, T. Senawong, *et al.*, 2004 Sirt1 promotes fat
910 mobilization in white adipocytes by repressing PPAR-gamma. *Nature* 429: 771–776.
911 <https://doi.org/10.1038/NATURE02583>

912 Prakash S., J. C. Caldwell, D. F. Eberl, and T. R. Clandinin, 2005 *Drosophila* N-cadherin
913 mediates an attractive interaction between photoreceptor axons and their targets. *Nat.*
914 *Neurosci.* 2005 84 8: 443–450. <https://doi.org/10.1038/nn1415>

915 Prisco G. Di, V. Cavaliere, D. Annoscia, P. Varricchio, E. Caprio, *et al.*, 2013 Neonicotinoid
916 clothianidin adversely affects insect immunity and promotes replication of a viral pathogen
917 in honey bees. *Proc. Natl. Acad. Sci.* 110: 18466–18471.
918 <https://doi.org/10.1073/PNAS.1314923110>

919 Queitsch C., K. D. Carlson, and S. Girirajan, 2012 Lessons from model organisms: phenotypic
920 robustness and missing heritability in complex disease. *PLoS Genet* 8: e1003041.
921 <https://doi.org/10.1371/journal.pgen.1003041>

922 Rabelink T. J., B. M. van den Berg, M. Garsen, G. Wang, M. Elkin, *et al.*, 2017 Heparanase:
923 roles in cell survival, extracellular matrix remodelling and the development of kidney
924 disease. *Nat. Rev. Nephrol.* 2017 134 13: 201–212. <https://doi.org/10.1038/nrneph.2017.6>

925 Rao Y., P. Pang, W. Ruan, D. Gunning, and S. L. Zipursky, 2000 brakeless is required for
926 photoreceptor growth-cone targeting in *Drosophila*. *Proc. Natl. Acad. Sci.* 97: 5966–5971.
927 <https://doi.org/10.1073/PNAS.110135297>

928 Reis T., M. R. Van Gilst, and I. K. Hariharan, 2010 A Buoyancy-Based Screen of *Drosophila*
929 Larvae for Fat-Storage Mutants Reveals a Role for Sir2 in Coupling Fat Storage to Nutrient
930 Availability, (E. Rulifson, Ed.). *PLoS Genet.* 6: e1001206.
931 <https://doi.org/10.1371/journal.pgen.1001206>

932 Rine J., and I. Herskowitz, 1987 Four Genes Responsible for a Position Effect on Expression
933 from HML and HMR in *Saccharomyces cerevisiae*. *Genetics* 116: 9.

- 934 Rodgers J. T., and P. Puigserver, 2007 Fasting-dependent glucose and lipid metabolic
935 response through hepatic sirtuin 1. *Proc. Natl. Acad. Sci. U. S. A.* 104: 12861–12866.
936 <https://doi.org/10.1073/pnas.0702509104>
- 937 Shannon P., A. Markiel, O. Ozier, N. S. Baliga, J. T. Wang, *et al.*, 2003 Cytoscape: a software
938 environment for integrated models of biomolecular interaction networks. *Genome Res.* 13:
939 2498–504. <https://doi.org/10.1101/gr.1239303>
- 940 Shlevkov E., and G. Morata, 2012 A dp53/JNK-dependant feedback amplification loop is
941 essential for the apoptotic response to stress in *Drosophila*. *Cell Death Differ.* 19: 451–460.
942 <https://doi.org/10.1038/cdd.2011.113>
- 943 Shore D., M. Squire, and K. A. Nasmyth, 1984 Characterization of two genes required for the
944 position-effect control of yeast mating-type genes. *EMBO J.* 3: 2817.
- 945 Sieber M. H., and C. S. Thummel, 2009 The DHR96 Nuclear Receptor Controls Triacylglycerol
946 Homeostasis in *Drosophila*. *Cell Metab.* 10: 481–490.
947 <https://doi.org/10.1016/J.CMET.2009.10.010>
- 948 Sivachenko A., H. B. Gordon, S. S. Kimball, E. J. Gavin, J. L. Bonkowsky, *et al.*, 2016
949 Neurodegeneration in a *Drosophila* model of adrenoleukodystrophy: the roles of the
950 Bubblegum and Double bubble acyl-CoA synthetases. *Dis. Model. Mech.* 9: 377–387.
951 <https://doi.org/10.1242/DMM.022244>
- 952 Somogyi K., B. Sipos, Z. Péntzes, and I. Andó, 2010 A conserved gene cluster as a putative
953 functional unit in insect innate immunity. *FEBS Lett.* 584: 4375–4378.
954 <https://doi.org/10.1016/J.FEBSLET.2010.10.014>
- 955 Spletter M. L., C. Barz, A. Yeroslaviz, C. Schönbauer, I. R. S. Ferreira, *et al.*, 2015 The RNA-
956 binding protein Arrest (Bruno) regulates alternative splicing to enable myofibril maturation
957 in *Drosophila* flight muscle. *EMBO Rep.* 16: 178–191.
958 <https://doi.org/10.15252/EMBR.201439791>
- 959 Subramanian A., P. Tamayo, V. K. Mootha, S. Mukherjee, B. L. Ebert, *et al.*, 2005 Gene set

960 enrichment analysis: a knowledge-based approach for interpreting genome-wide
961 expression profiles. *Proc. Natl. Acad. Sci. U. S. A.* 102: 15545–50.
962 <https://doi.org/10.1073/pnas.0506580102>

963 Talsness D. M., K. G. Owings, E. Coelho, G. Mercenne, J. M. Pleinis, *et al.*, 2020 A drosophila
964 screen identifies *nkcc1* as a modifier of *ngly1* deficiency. *Elife* 9: 1–22.
965 <https://doi.org/10.7554/ELIFE.57831>

966 Tennessen J. M., W. E. Barry, J. Cox, and C. S. Thummel, 2014 Methods for studying
967 metabolism in *Drosophila*. *Methods* 68: 105–115.
968 <https://doi.org/10.1016/j.ymeth.2014.02.034>

969 Udler M. S., M. I. McCarthy, J. C. Florez, and A. Mahajan, 2019 Genetic Risk Scores for
970 Diabetes Diagnosis and Precision Medicine. *Endocr. Rev.* 40: 1500–1520.
971 <https://doi.org/10.1210/er.2019-00088>

972 Wu H., and C. M. Ballantyne, 2020 Metabolic Inflammation and Insulin Resistance in Obesity.
973 *Circ. Res.* 126: 1549. <https://doi.org/10.1161/CIRCRESAHA.119.315896>

974 Yang J., X. Kong, M. Martins-Santos, G. Aleman, E. Chaco, *et al.*, 2009 Activation of SIRT1 by
975 resveratrol represses transcription of the gene for the cytosolic form of
976 phosphoenolpyruvate carboxykinase (GTP) by deacetylating hepatic nuclear factor 4alpha.
977 *J. Biol. Chem.* 284: 27042–27053. <https://doi.org/10.1074/JBC.M109.047340>

978 Zhao Y., J. Wei, X. Hou, H. Liu, F. Guo, *et al.*, 2017 SIRT1 rs10823108 and FOXO1
979 rs17446614 responsible for genetic susceptibility to diabetic nephropathy. *Sci. Reports*
980 2017 7: 1–9. <https://doi.org/10.1038/s41598-017-10612-7>

981 Zhou X., and M. Stephens, 2012 Genome-wide efficient mixed-model analysis for association
982 studies. *Nat. Genet.* 44: 821–4. <https://doi.org/10.1038/ng.2310>

983 Zhou X., C. J. Guo, H. H. Hu, J. Zhong, Q. Sun, *et al.*, 2019 *Drosophila* CTP synthase can form
984 distinct substrate- and product-bound filaments. *J. Genet. Genomics* 46: 537–545.
985 <https://doi.org/10.1016/J.JGG.2019.11.006>

986 Zillikens M. C., J. B. J. van Meurs, F. Rivadeneira, N. Amin, A. Hofman, *et al.*, 2009 SIRT1

987 Genetic Variation Is Related to BMI and Risk of Obesity. *Diabetes* 58: 2828–2834.

988 <https://doi.org/10.2337/DB09-0536>

989

990

FIGURE LEGENDS

991 **Figure 1. Glucose levels vary under a variety of environmental conditions.**

992 Glucose levels were measured in three samples for each of 30-36 strains under one of the
993 indicated conditions: one week of adult age and fed ad libitum (N = 30 strains, P = 1.87E-05)
994 (A), one week of adult age and fasted for 12-13 hours (N = 30 strains, P = 0.0194) (B), two
995 weeks of adult age and fed ad libitum (N = 30 strains, P = 0.0103) (C), and two weeks of adult
996 age and fasted for 12-13 hours (N = 36 strains, P = 1.95E-05) (D). Mean glucose concentrations
997 are indicated, with error bars indicating standard deviation. DGRP strain or RAL numbers are
998 indicated along the X-axis. P-values were calculated using one-way ANOVA incorporating all
999 individual measurements comparing DGRP strain with glucose concentration. Adult flies were
1000 collected within 2-3 days after eclosion from the pupal case and aged to the indicated time
1001 points. * P < 0.05, **** P < 5E-05.

1002

1003 **Figure 2. Glucose levels are significantly affected by genetic background.**

1004 Glucose levels were measured in three samples for each of 185 strains at two weeks of age
1005 after a 12 hour fast. Adult flies were collected within 2-3 days after eclosion from the pupal case
1006 and aged an additional 9-11 days prior to fasting (11-14 days post-eclosion). Flies were
1007 collected after the overnight fast at 12-15 days post-eclosion. Mean glucose concentrations are
1008 indicated, with error bars indicating standard deviation. P-values were calculated using one-way
1009 ANOVA incorporating all individual measurements comparing DGRP strain with glucose
1010 concentration (P < 2E-16).

1011

1012 **Figure 3. Immune responses, neuronal function, and basic metabolic processes are**
1013 **overrepresented in GWA candidate modifiers of hyperglycemia.**

1014 **(A)** *R4>Sirt1i* modifier network, as plotted by the GeneMANIA plugin in Cytoscape (Shannon *et*
1015 *al.* 2003; Montojo *et al.* 2010). Significant candidate modifiers are indicated in red, with physical
1016 interactions indicated by connecting red lines. Thicker lines indicate stronger evidence for the
1017 interaction. Encircled genes share common pathways or functions. Interacting genes outside of
1018 the candidate modifier list are indicated in gray. **(B)** Top 20 significant ontological categories as
1019 identified by GSEA. Categories are arranged from most significant on top to least significant
1020 along the y-axis. P-values are indicated by red-to-blue gradient, with red the lowest p-values
1021 and blue the highest P-values. Enrichment score (ES) for each category is plotted along the x-
1022 axis. Gene number identified in each category is indicated by dot size.

1023

1024 **Figure 4. Loss of candidate gene expression suppresses hyperglycemia in the *R4>Sirt1i***
1025 **model**

1026 RNAi against candidate modifiers was expressed under the control of *R4-GAL4* in the *R4>Sirt1i*
1027 model. Glucose level for each sample was normalized to the levels in a genetically matched
1028 control line crossed into the *R4-Sirt1* line. Average *R4>Sirt1i* control glucose levels after
1029 normalization are indicated by a dotted line at 1.0, with standard deviation highlighted by the gray
1030 box. Whole fly glucose concentration was quantified for N = 4-5 samples per strain, each
1031 consisting of 5 flies and individually plotted along the y-axis. Knockdown of *CG4168*, *CG5888*, or
1032 *uif* significantly reduces glucose concentrations in the *R4>Sirt1i* model of hyperglycemia
1033 compared to controls (blue). Loss of *CTPSyn* does not significantly alter glucose levels, but a
1034 trending decrease in glucose levels were observed in several independent RNAi strains (light
1035 blue, data not shown). Loss of *smt3*, *ilp5*, *snRNP-U1-70k*, *CG10265*, *CG15803*, *Roe*, *CG34353*,
1036 *CadN2*, *CG43897*, *CG3407*, *dsxc73A*, or *bgm* do not produce a significant effect (dark gray). P-

1037 values were calculated using one-way ANOVA followed by Dunnett's multiple testing correction.

1038 * P < 0.05, *** P < 0.001.

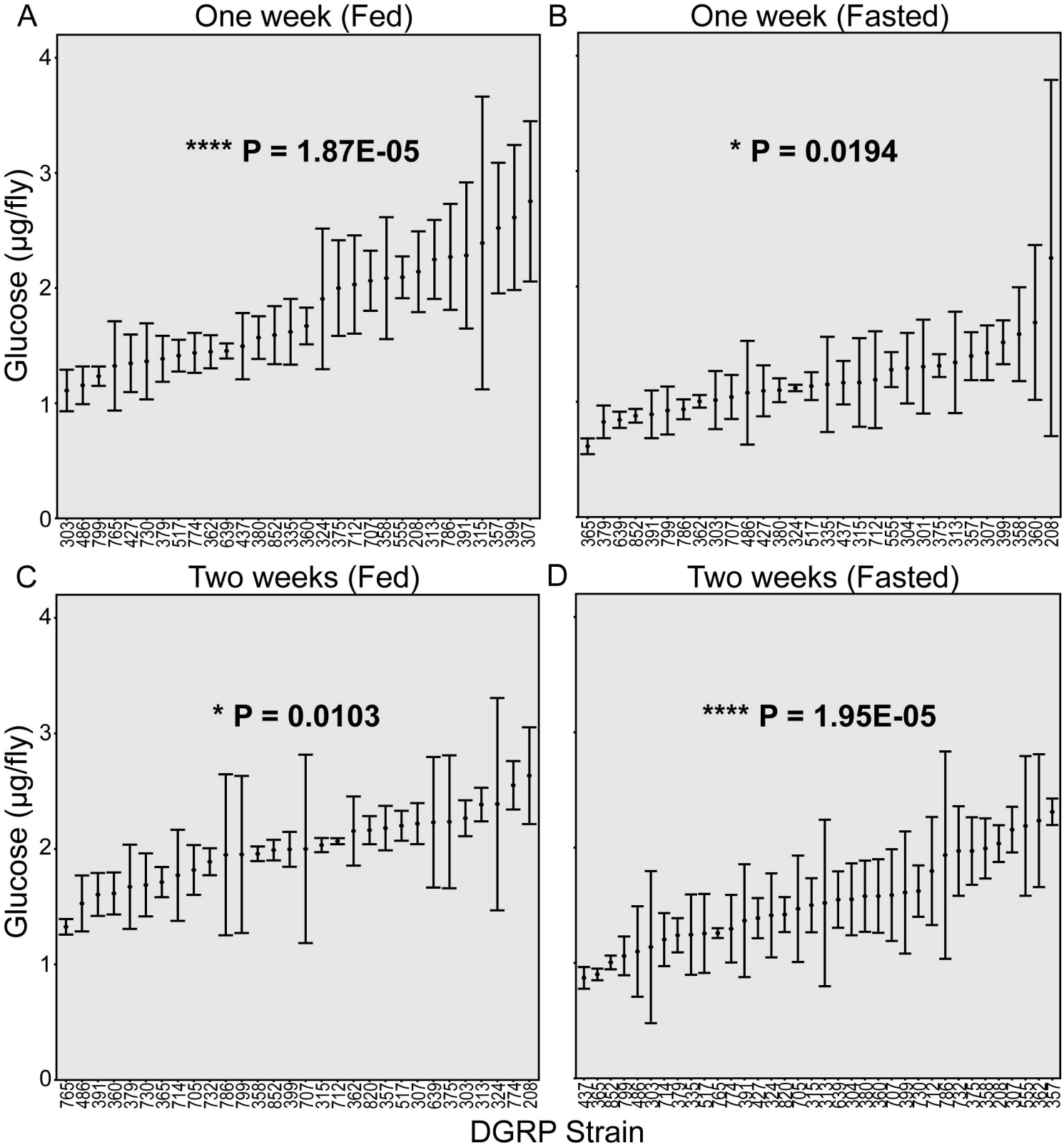


Figure 1.

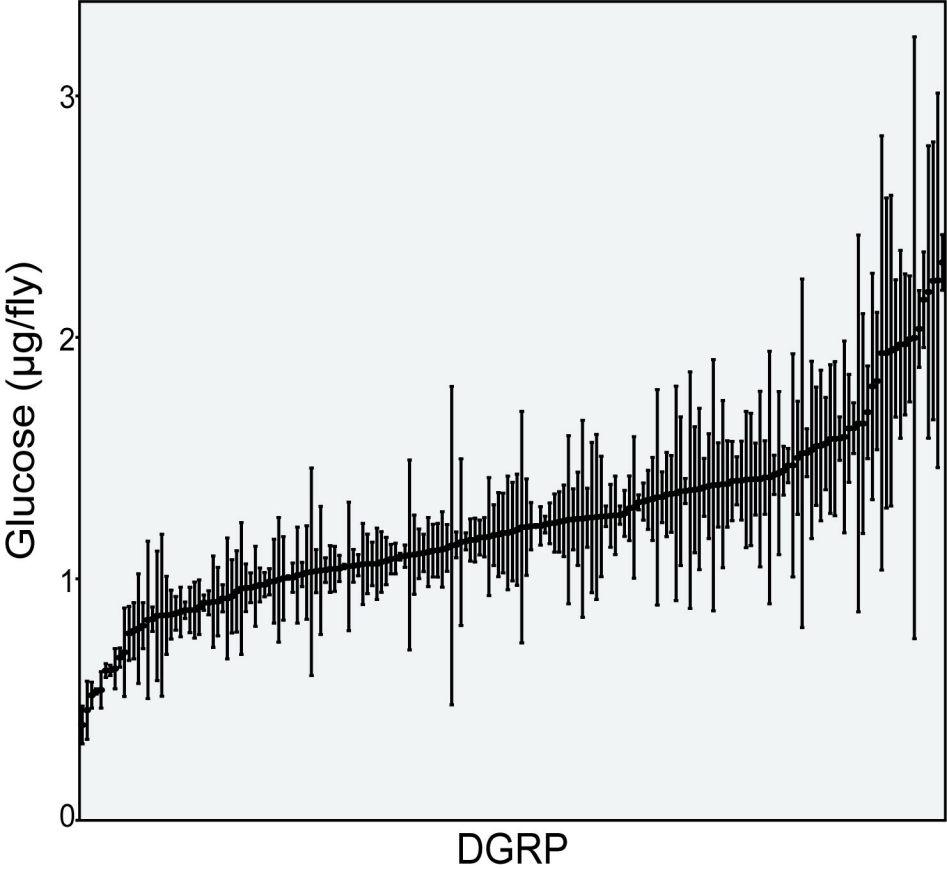


Figure 2

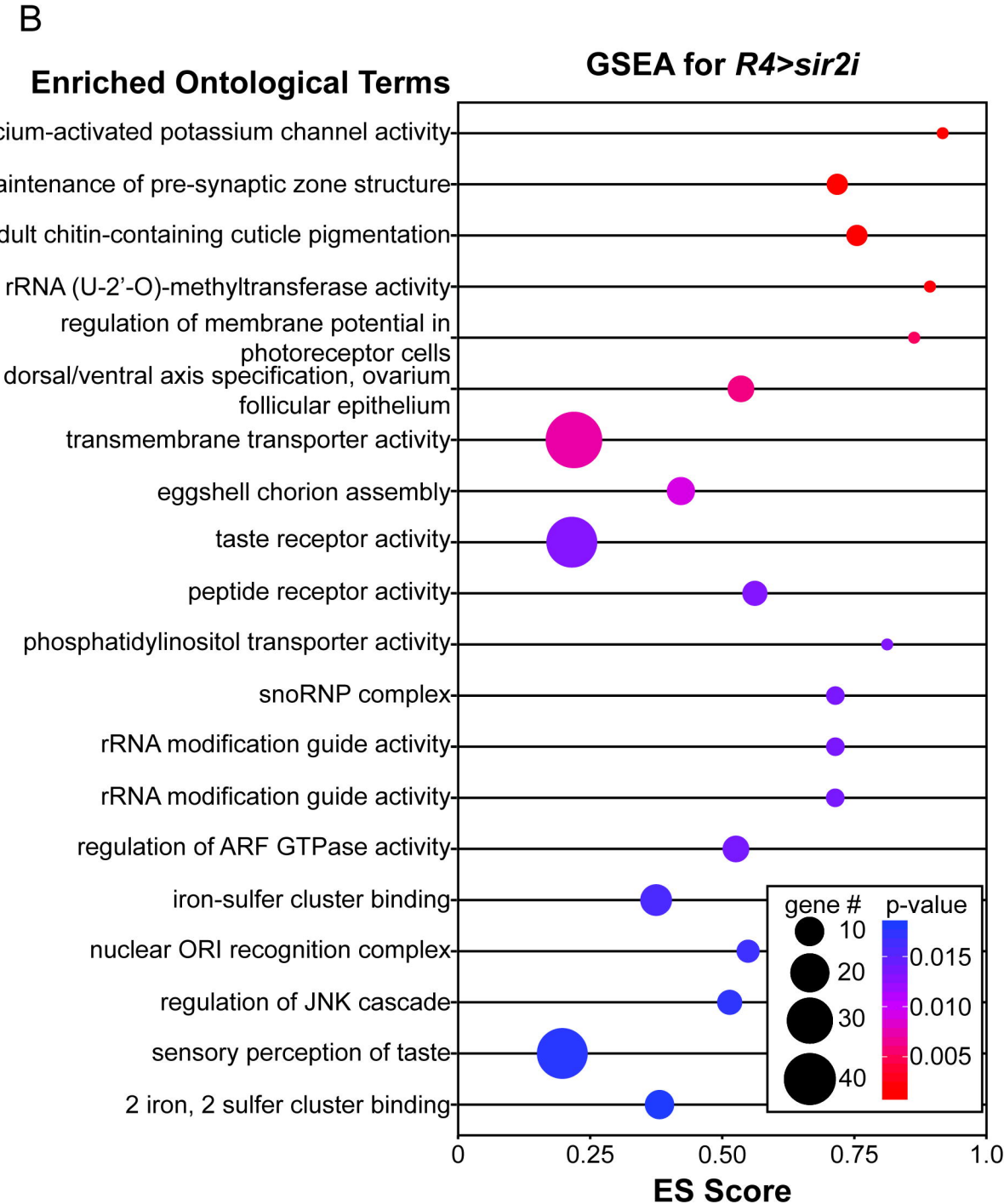
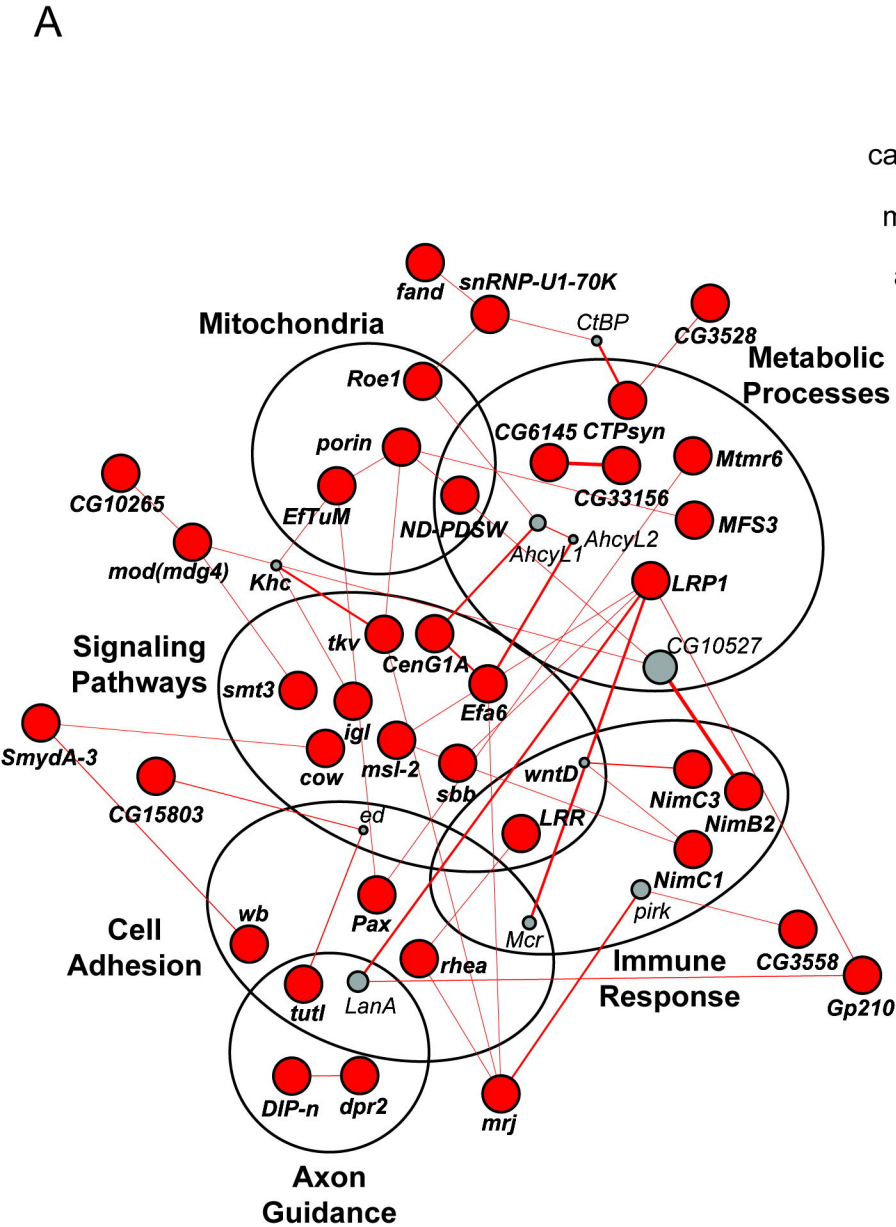


Figure 3

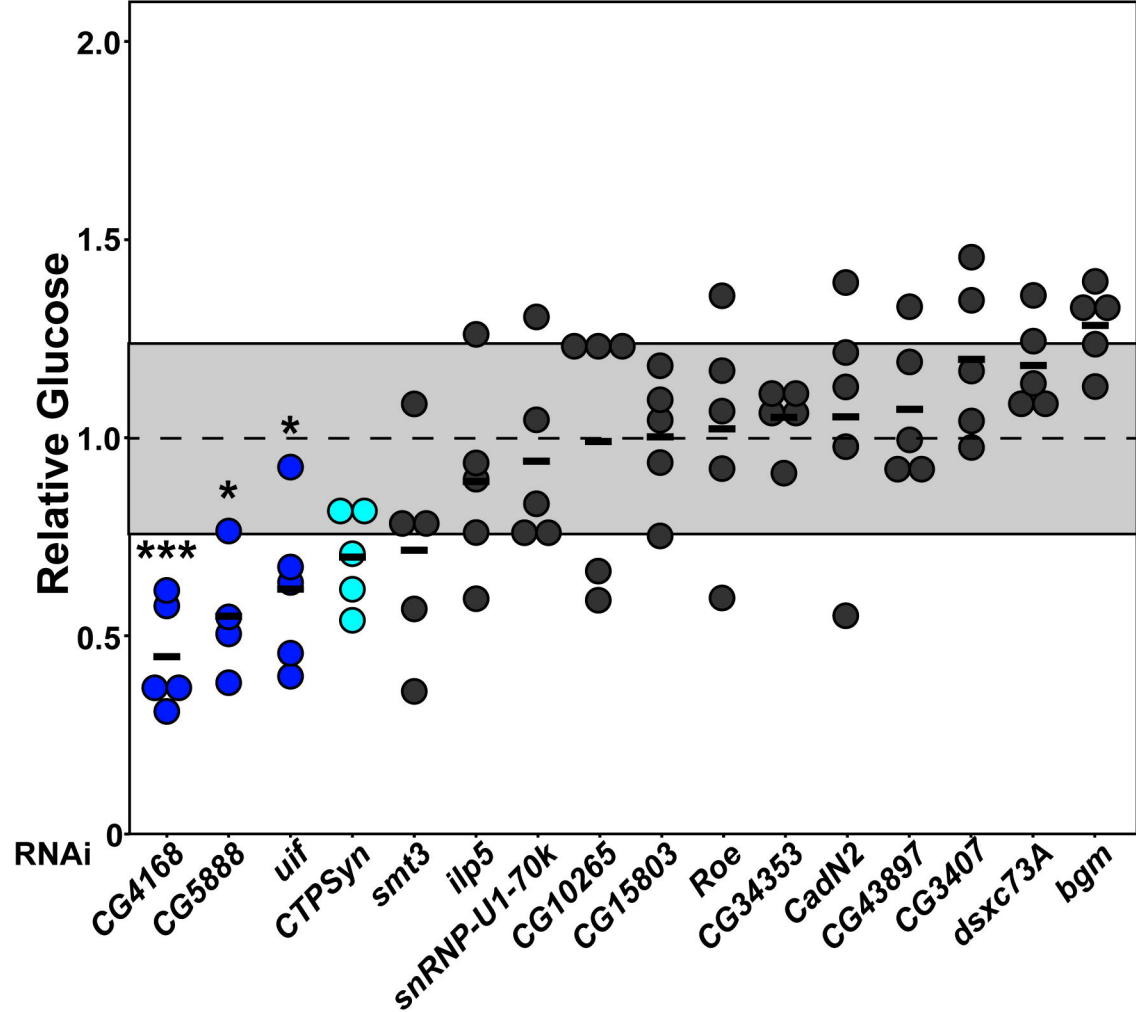


Figure 4